



DIPLOMARBEIT

Titel der Diplomarbeit

Osteomacrophages in Cathepsin S Knockout Mice

Verfasserin

Nadine Jasmin Ortner

angestrebter akademischer Grad

Magistra der Naturwissenschaften (Mag.rer.nat.)

Wien, 2012

Studienkennzahl lt. Studienblatt:

A 490

Studienrichtung lt. Studienblatt:

Diplomstudium der Molekularen Biologie

Betreuerin / Betreuer:

Univ.-Prof. Mag. Dr. Pavel Kovarik

Acknowledgements

It is a big pleasure for me to thank all the people who made this diploma thesis possible.

First of all I want to thank M.D., Assoc. Professor **Peter Pietschmann**, the supervisor of my diploma thesis project, for teaching and supporting me during this time. He not only always found the time for listening to me and giving helpful advice, he also gave me the opportunity to work quiet autonomously and therefore to establish valuable experience and job-related confidence. Moreover I want to thank the Department of Pathophysiology and Allergy Research (Center of Pathophysiology, Infectiology and Immunology, **Medical University of Vienna**) and the **Austrian Science Fund (FWF)** for providing the material and equipment for this project (# P 20239-B13), as well as Ass. Prof. Dr. **Harald Höger** for the breeding and care of the mice.

Special thanks go to my colleges, BSc. **Andrea Kapfenberger**, Mag. **Ursula Föger-Samwald**, Ing. **Katharina Wahl** and **Birgit Schwarz**. Next to showing me tips and tricks of many techniques in the laboratory, they also made my time in this department not only nicer but really a great pleasure and big fun. I will miss our coffee breaks and all the numerous laughing fits so much.

I also owe thanks to **Erika Bajna** and **Hana Uhrova**, who patiently helped me expanding and improving my skills in immunohistochemistry. And again thanks to BSc. **Andrea Kapfenberger** for performing the genotyping of the animals.

Last but not least I want to thank **Michael Stanschitz** for always listening to my worries and helping me to gather new energy. And of course more than just special thanks to my parents, **Elisabeth** and **Hans Ortner**, for not giving up supporting my scientific education in all these years.

Hey, it's done!

Table of contents

Acknowledgements	- 1 -
Table of contents	- 2 -
Summary	- 3 -
Zusammenfassung	- 4 -
Introduction	- 6 -
<i>Bone</i>	<i>- 6 -</i>
<i>Osteoblasts</i>	<i>- 7 -</i>
<i>Osteocytes</i>	<i>- 9 -</i>
<i>Bone lining cells</i>	<i>- 10 -</i>
<i>Osteoclasts</i>	<i>- 11 -</i>
<i>Bone remodeling</i>	<i>- 12 -</i>
<i>Macrophages</i>	<i>- 13 -</i>
<i>Osteomacs</i>	<i>- 14 -</i>
<i>Proposed model of the role of osteomacs in bone modeling</i>	<i>- 15 -</i>
<i>Proposed model of the role of osteomacs in bone remodeling</i>	<i>- 16 -</i>
<i>Cathepsin S</i>	<i>- 17 -</i>
Hypothesis / Aim of the study	- 18 -
Materials	- 19 -
<i>Reagents</i>	<i>- 19 -</i>
<i>Sera</i>	<i>- 20 -</i>
<i>Antibodies & Stains</i>	<i>- 20 -</i>
<i>Solutions</i>	<i>- 21 -</i>
Methods	- 23 -
<i>Animals</i>	<i>- 23 -</i>
<i>Paraffin embedding</i>	<i>- 23 -</i>
<i>Sectioning</i>	<i>- 23 -</i>
<i>Immunohistochemistry</i>	<i>- 24 -</i>
<i>Cell culture</i>	<i>- 25 -</i>
<i>Flow cytometry</i>	<i>- 25 -</i>
<i>Micro-computed tomography</i>	<i>- 26 -</i>
<i>Histomorphometry</i>	<i>- 26 -</i>
<i>Statistical Analysis</i>	<i>- 27 -</i>
Results	- 28 -
<i>Visualization of F4/80 positive cells</i>	<i>- 28 -</i>
<i>Investigation of MHC II expression</i>	<i>- 31 -</i>
<i>Alteration in bone microarchitecture</i>	<i>- 34 -</i>
<i>Examination of osteocyte lacunae</i>	<i>- 37 -</i>
Discussion	- 41 -
<i>Presence and distribution of osteomacs</i>	<i>- 41 -</i>
<i>Number of osteomacs / bone marrow macrophages</i>	<i>- 42 -</i>
<i>MHC class II expression</i>	<i>- 43 -</i>
<i>Bone microarchitecture</i>	<i>- 45 -</i>
<i>Strengths and limitations</i>	<i>- 46 -</i>
<i>Conclusion</i>	<i>- 47 -</i>
References	- 49 -
Abbreviations	- 55 -
List of figures	- 58 -
List of tables	- 59 -
Curriculum vitae	- 60 -

Summary

Background: Resident tissue macrophages are present in nearly every tissue of the body, where they fulfill global as well as tissue adapted functions. In bone tissue, they are called osteomacs. These cells play an important role in the support of bone formation and immune surveillance. Cathepsin S is a lysosomal protease that is involved in several cellular processes such as extracellular matrix (ECM) remodeling and antigen processing and presentation. Furthermore, cathepsin S influences the differentiation of mesenchymal stem cells (MSCs), the progenitors of the bone forming osteoblasts, as it favors their development towards the adipocyte lineage.

Aim: In the present study, we investigated the possible influence of cathepsin S deficiency on osteomacs. We hypothesized a reduced number of F4/80⁺ macrophages, a decline in MHC (major histocompatibility complex) class II expression on these cells and a discreet bone phenotype.

Methods: The presence and distribution of osteomacs in the spine of cathepsin S knockout and wild-type mice were determined by immunofluorescence stainings, using a monoclonal antibody against the surface molecule F4/80. The number of F4/80⁺ macrophages and their MHC class II expression were examined by flow cytometry analyses. Histomorphometric and micro-computed tomography measurements of the 5th lumbar vertebra were performed to evaluate alterations in the bone microarchitecture.

Main results: In both mouse genotypes the number of F4/80⁺ cells was similar. Numerically cathepsin S knockout mice displayed an increased mean fluorescence intensity of the MHC II signal. Additionally, we found less mineralized bone tissue, thinner trabeculae and smaller osteocyte lacunae in the knockout mice.

Conclusion: Cathepsin S deficient mice show a reproducible bone phenotype and evidence of macrophage activation. Currently pharmacologic inhibitors of cathepsin S are proposed for the treatment of obesity and several immune disorders; based on our findings we strongly advice to monitor bone turnover and bone mineral density in patients treated with cathepsin S inhibitors.

Zusammenfassung

Hintergrund: Residente Gewebsmakrophagen sind in fast jedem Gewebe des Körpers vorhanden, wo sie sowohl globale als auch an das Gewebe angepasste Funktionen erfüllen. Diese Zellen werden im Knochen „Osteomakrophagen“ genannt und spielen bei der Unterstützung der Knochenneubildung und Immunüberwachung eine wichtige Rolle. Cathepsin S ist eine lysosomale Protease, welche bei verschiedenen zellulären Prozessen, wie zum Beispiel dem Remodelling der extrazellulären Matrix oder der Antigenprozessierung und –präsentation, eine wichtige Rolle spielt. Darüber hinaus beeinflusst Cathepsin S die Differenzierung von mesenchymalen Stammzellen (von denen auch die Osteoblasten abstammen) da es deren Entwicklung in Richtung der Adipozyten begünstigt.

Ziel: Ziel dieser Studie war es zu untersuchen, ob die Cathepsin S Defizienz die Osteomakrophagen beeinflusst. Die der Arbeit zugrunde liegenden Hypothesen waren eine reduzierte Anzahl von F4/80⁺ Makrophagen, eine Abnahme der Hauptkompatibilitätskomplex (MHC) Klasse II Expression und ein dezenter Knochen-Phänotyp.

Methoden: Die Anwesenheit und Verteilung von Osteomakrophagen in der Wirbelsäule von Cathepsin S Knockout- und Wildtyp-Mäusen wurde durch Immunfluoreszenz-Färbungen mit einem monoklonalen Antikörper gegen das Oberflächenmolekül F4/80 festgestellt. Die Anzahl der F4/80⁺ Makrophagen und deren MHC Klasse II Expression wurde mittels der Durchflusszytometrie untersucht. Zur Feststellung von Veränderungen der Knochenmikroarchitektur wurden histomorphometrische und mikro-Computertomographie Messungen des fünften Lendenwirbelkörpers durchgeführt.

Resultate: In beiden Maus Genotypen waren Anzahl und Verteilung der F4/80⁺ Zellen gleich. Numerisch wiesen Cathepsin S Knockout Mäuse eine erhöhte Mean Fluorescence Intensity des MHC Klasse II Signals auf. Zusätzlich wurden ein vermindert mineralisiertes Knochengewebe, dünnere Trabekel und kleinere Osteozyten-Lakunen bei den Knockout Mäusen gefunden.

Schlussfolgerung: Cathepsin S defiziente Mäuse zeigen einen reproduzierbaren Knochen-Phänotyp und Hinweise auf Makrophagen-Aktivierung. Derzeit werden pharmakologische Cathepsin S Inhibitoren zur Behandlung der Adipositas und verschiedener immunologischer Erkrankungen diskutiert; basierend auf unseren Ergebnissen raten wir dringend zu einer Überwachung des Knochenstoffwechsels und der Knochendichte bei Patienten, welche mit Cathepsin S Inhibitoren behandelt werden.

Introduction

Bone

In general, bone fulfills fundamental physical functions like supporting the constitution of the body, protecting the organs of an organism and enabling locomotion. In addition, bone is also very important for several processes on a more cellular and metabolic level. For instance, it serves as a mineral reservoir and provides a niche for haematopoietic stem cells (HSCs) [1]. Thus it is crucial for the formation of the cellular components of the blood including cells of the immune system [2].

Bone is a strong, stable and highly organized tissue, but to be able to accomplish all its functions, it also has to be very dynamic and flexible. Therefore, it undergoes constant rebuilding to adjust itself to environmental changes and mechanical impacts. The basic concept of this two-edged characteristic can be found in the composition of this tissue. The mechanical strength and stability is achieved by the bone mineral that is mainly composed of hydroxyapatite crystals $[\text{Ca}_{10}(\text{PO}_4)_6(\text{OH})_2]$. In contrast, the organic matrix, consisting primarily of type I collagen and additional other non collagenous proteins, is responsible for the elastic and flexible nature of bone [1].

Moreover, bone can be divided into two major types of bone tissue, the compact or cortical bone and the cancellous or trabecular bone. The cortical bone tissue builds up the outward layer of the bone and is very dense and stiff. On the contrary, the cancellous bone can be found on the inside where it is arranged in a complex, honeycomb-like network that harbors the bone marrow [1].

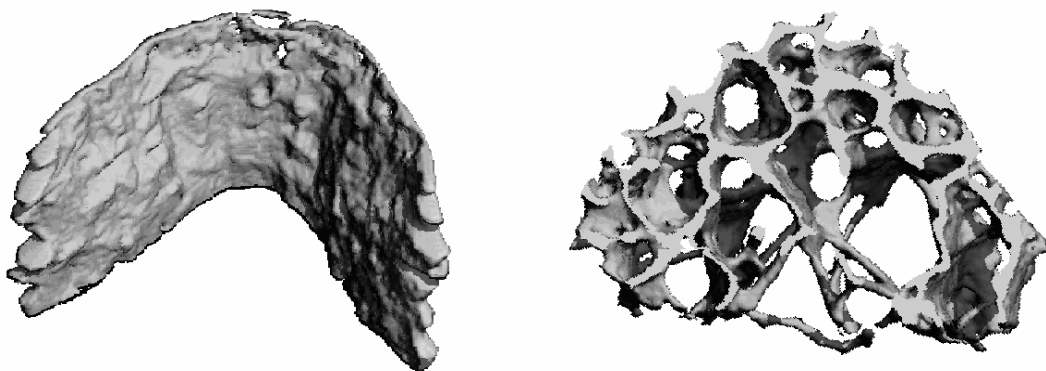


Figure 1: Cortical (left) and trabecular (right) bone of a murine vertebral body. 3D models were assembled out of 231 scanned slices of a micro-computed tomography (μ -CT) measurement.

The inner and outer surface of the bone is coated by a thin layer that contains the main bone cell types. On the inside it is called endosteum, a one to two cells thick membrane that is in direct contact with the bone marrow. The periosteum on the outside is thicker and exhibits next to the inner cellular layer an additional dense fibrous layer [1, 3].

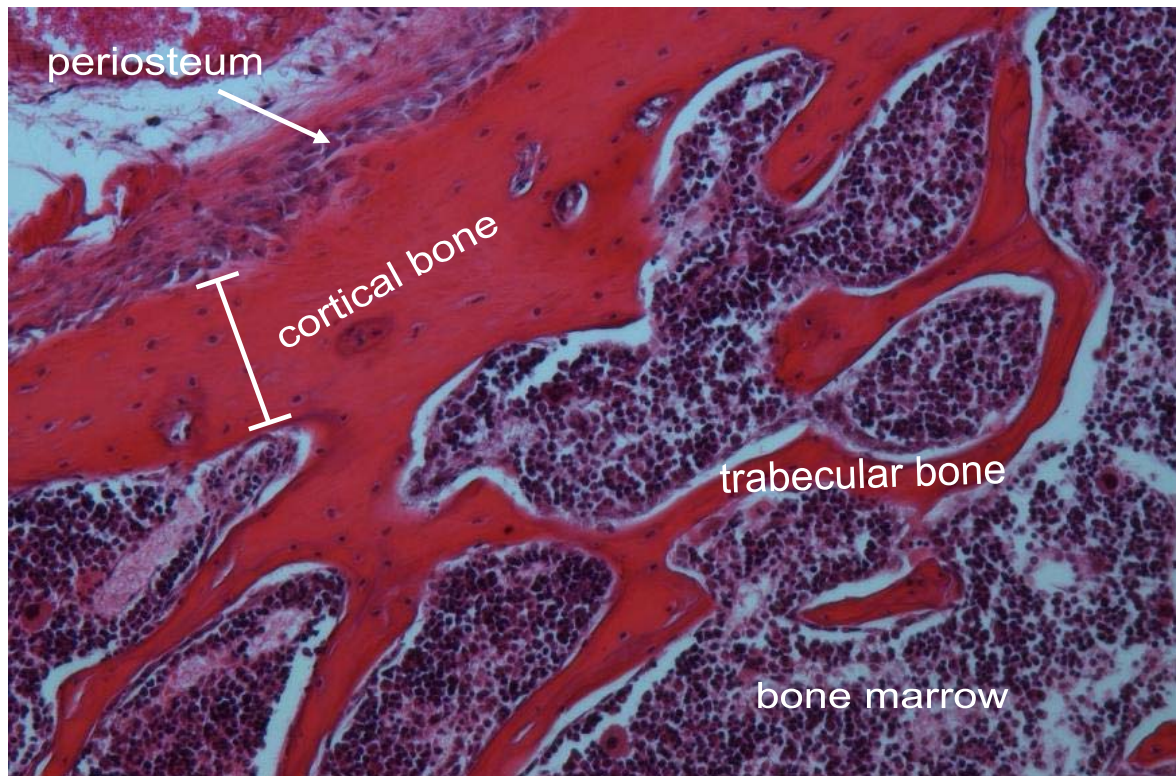


Figure 2: Hematoxylin and eosin (HE) staining of a murine vertebral body (original magnification: 10x). Spine of a female, three months old HIM:OF-1 mouse was fixed in 4 % paraformaldehyde (PFA), decalcified and embedded in paraffin. HE staining was performed on 4 μ m thick sections. Nuclei are shown in purple, cytoplasm and bone matrix occur in red.

Osteoblasts

Osteoblasts are responsible for the formation of bone. They derive from mesenchymal stem cells (MSCs) that differentiate into osteoprogenitor cells. These cells are the source for osteoblasts, osteocytes as well as bone lining cells [4, 5]. Upon activation, they start to synthesize and secrete new, unmineralized bone matrix components (osteoid). Subsequently, they catalyze and regulate its mineralization. These metabolic processes are accompanied by a morphological change, as shown in Figure 3. Active osteoblasts become round, cuboidal and polarized [for review see 1].

Moreover, cells derived from osteoprogenitor cells are able to interact with the bone degrading osteoclasts. By producing osteoclastogenic factors such as macrophage colony-stimulating factor (M-CSF), receptor activator of nuclear factor- κ B ligand (RANKL) and osteoprotegerin (OPG), they contribute to the recruitment and differentiation process of osteoclasts [6, 7].

The soluble M-CSF is crucial for the maturation and survival of cells of the monocyte-macrophage cell line [8]. This is achieved by the activation of the colony stimulating factor-1 (CSF-1) receptor that is also present on osteoclasts. RANKL initiates osteoclastogenesis by binding to the receptor activator of NF- κ B (RANK) on the osteoclast surface. This interaction can be prevented by the osteoblastic expression of OPG, a soluble competitor of RANKL. Thus, osteoblasts can control osteoclast differentiation and activity by the regulation of the amount of RANKL and its decoy receptor OPG [for review see 9, 10].

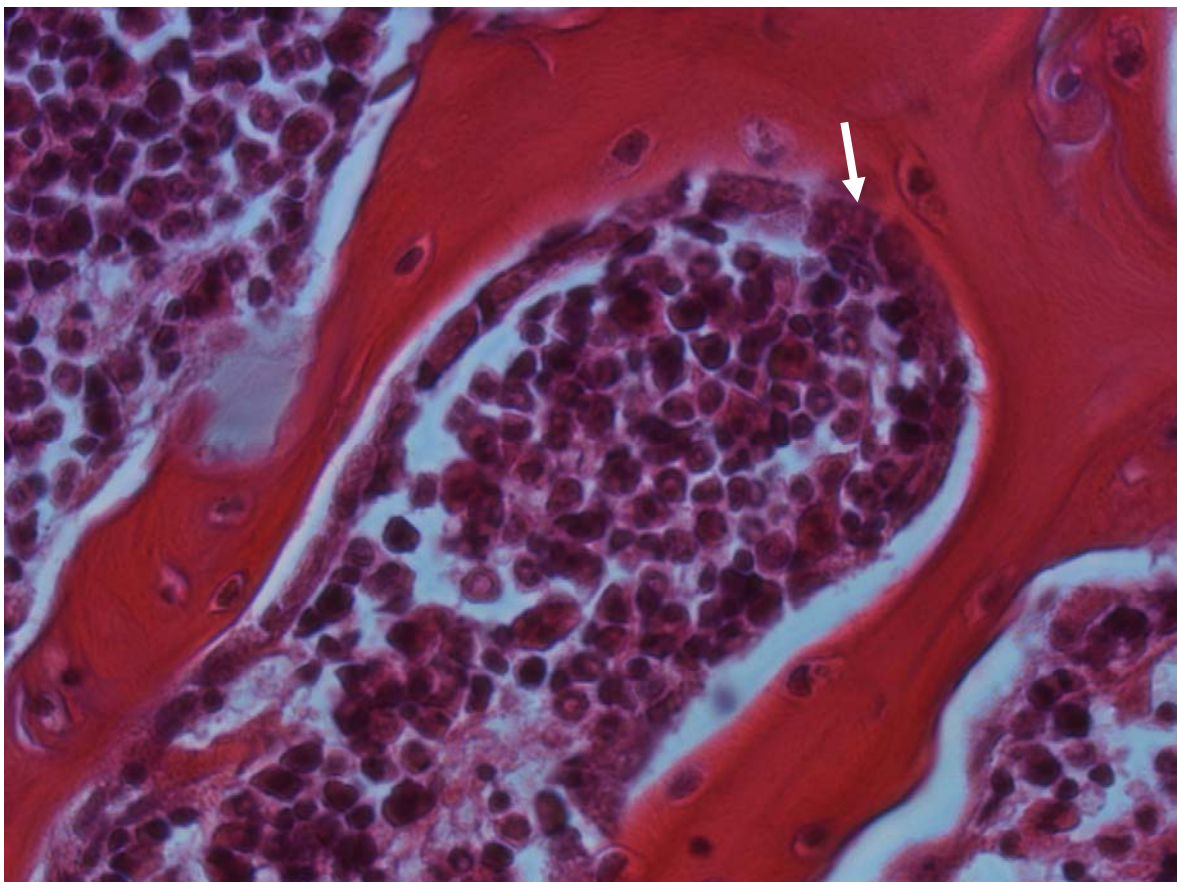


Figure 3: HE stained section of a murine vertebra showing active, cuboidal osteoblasts (original magnification: 40x). Vertebral column was fixed in 4 % PFA, decalcified for 5 days in Tris/EDTA and finally embedded in paraffin. Four μ m thick sections were stained with hemalum and eosin Y.

Osteocytes

Active osteoblasts synthesize and secrete osteoid and regulate its subsequent mineralization. During bone formation, a part of them gets gradually surrounded and finally trapped within the mineralized bone matrix. They change their morphology from cuboidal to more stellate-shaped and differentiate into fully mature osteocytes [11, 12].

With their long processes inside interconnecting channels, the so called canaliculi, they build up a huge network throughout the whole bone. Via gap junctions they keep contact with other engulfed osteocytes, each lying in its distinct lacunae, as well as with osteoblasts and bone lining cells at the bone surface. This complex lacunocanicular system enables an exchange of nutrients and information [12, 13].

As a result, they can forward information they get through mechanosensation [14] to other bone cells and thereby contribute to the coordination of bone structure and turnover.

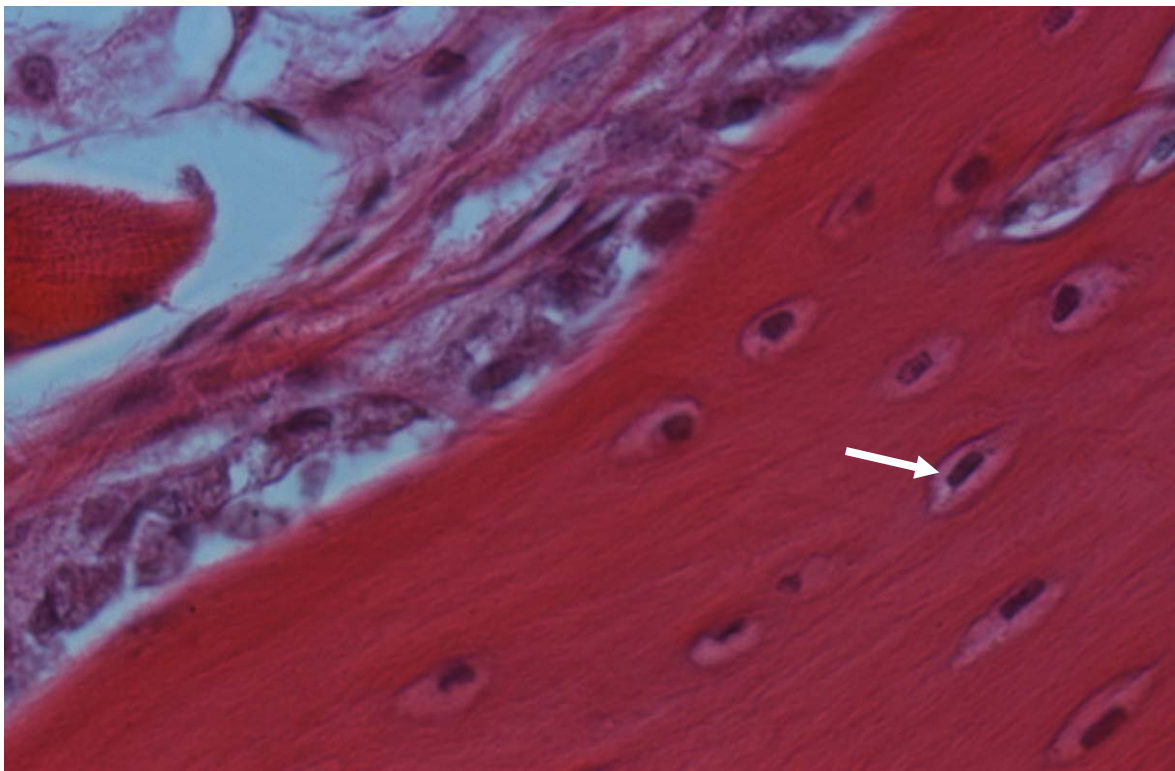


Figure 4: Osteocytes lying in individual lacunae in a HE stained section of a murine vertebral column (original magnification: 40x). Spines were prepared as described in Figures 2 and 3. Cytoplasm and bone matrix are shown in red, nuclei occur purple.

Bone lining cells

The bone lining cells mainly build up the cellular part of the endosteum and periosteum and cover the bone if it is in a quiescent state. Like osteoblasts and osteocytes, they derive from osteoprogenitor cells with mesenchymal origin [1].

If bone remodeling occurs, they retreat or redifferentiate into active, osteoid-producing osteoblasts. Moreover, they may participate in the preparation of the bone surface prior the onset of bone resorption [15] and bone formation [16] during bone remodeling. Thus, they can participate in bone dynamics and subsequently contribute to bone integrity.

In addition, these thin and elongated cells form a kind of protective barrier on the bone surface. As a result, they may be involved in mineral homeostasis by regulating the exchange of mineral ions between the bone and its environment [17].

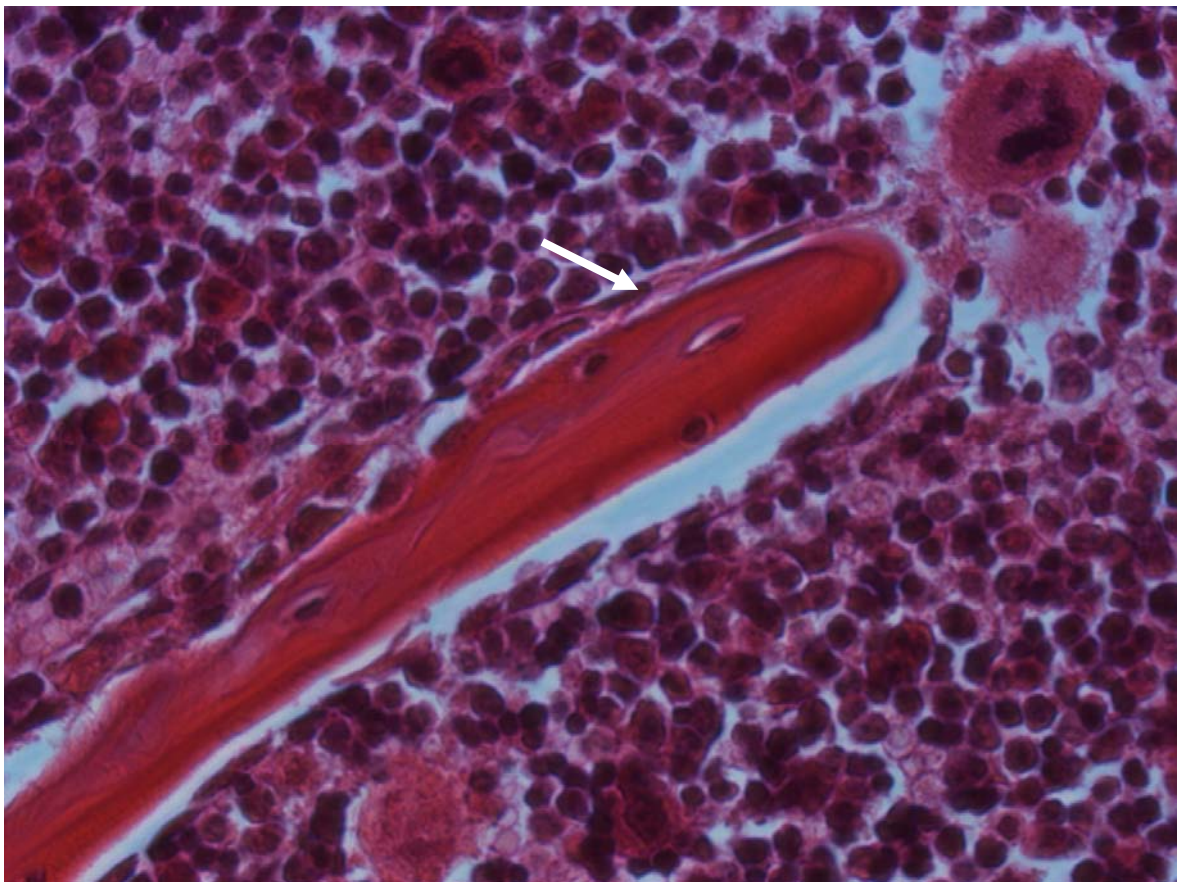


Figure 5: Bone lining cells in a HE stained section of a murine vertebral column (original magnification: 40x). Spines were prepared as described in Figures 2 and 3. Cytoplasm and bone matrix occur red, nuclei are stained purple.

Osteoclasts

Osteoclasts are of haematopoietic origin and develop along the myeloid lineage [18, 19]. They degrade bone tissue by breaking down the mineralized matrix and resorbing its liberated components. The recruitment and activation of osteoclast precursors is regulated via factors like M-CSF, RANKL and OPG. These molecules can be synthesized by osteoblasts and osteoblastic stromal cells, in response to a variety of factors such as parathyroid hormone (PTH), parathyroid hormone-related peptide (PTHrP), tumor necrosis factor- α (TNF- α) and interleukin-1 (IL-1) [6].

Upon activation, the osteoclast precursors of the monocyte-macrophage lineage fuse to form large, multinucleated cells. These polykaryons become polarized and form a specialized compartment at the bone facing site that is isolated by an actin sealing ring. Here, they start to secrete proteolytic enzymes and hydrogen chloride (HCl). As a result of the acidification within this resorption cavity, bone mineral gets dissolved. On the other hand, the organic matrix gets degraded by the secreted collagenolytic enzymes such as cathepsin K and matrix metalloproteinases. Released matrix components are subsequently removed via transcytosis to the non bone facing site of the osteoclast [for review see 18].

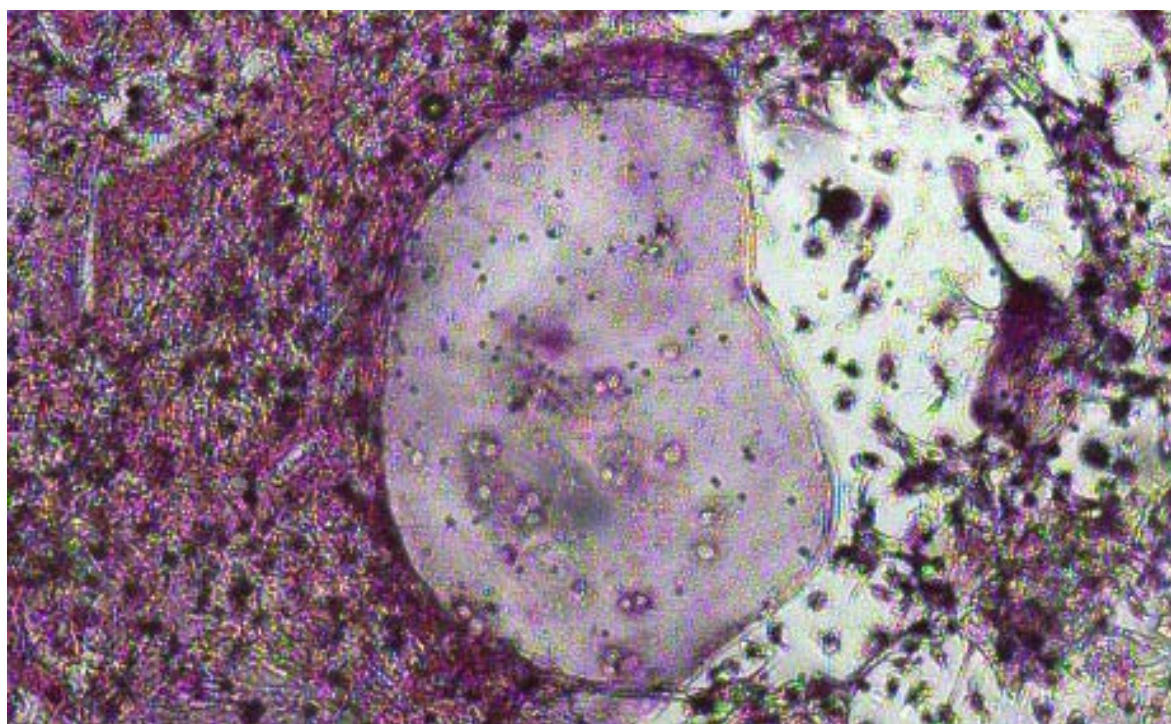


Figure 6: A multinucleated TRAP-stained osteoclast in a bone marrow culture (original magnification: 10x). Bone marrow cells were incubated for one week in standard medium containing 10^{-8} M $1,25(\text{OH})_2\text{D}_3$ (37 °C, % CO_2 and 95 % air humidity). Medium was changed every 3 days. Cells were stained for TRAP using the Leukocyte Acid Phosphatase Kit (Sigma 387A-1KT). TRAP = tartrate-resistant acid phosphatase

Bone remodeling

Bone remodeling is a highly coordinated metabolic process that involves the action of bone forming osteoblasts and bone degrading osteoclasts. The maintenance of the overall bone mass is ensured by the strict coupling of the activity of these two bone cells. This dynamic process takes place at the inner and outer bone surface in response to mechanical impacts, microdamages or metabolic stimuli [1, 6].

A remodeling cycle starts with the recruitment of preosteoclasts that develop from the monocyte-macrophage lineage. The expression of M-CSF, RANKL and OPG by osteoblasts and bone marrow stromal cells subsequently drives the fusion and differentiation to mature, multinucleated osteoclasts. Attachment of osteoclasts is enabled by the removal of unmineralized osteoid from the bone surface by bone lining cells [15]. During bone degradation, osteoclasts get polarized and display several distinct membrane domains. At the bone facing site is the ruffled border, encircled by the sealing zone (actin ring) that enables the establishment of an isolated compartment. Here, collagenolytic enzymes and hydrogen chloride (HCl) are released and dissolve the mineralized bone matrix. Degradation remnants are removed from the resorption cavity by endocytosis. Subsequently, the endocytosed vesicles are transported to the non bone facing site of the osteoclast and released at the secretory domain [for review see 18].

The activation and resorption phase of the remodeling cycle is followed by the so called reversal phase. During this phase, yet unknown mononuclear cells clean the bone surface. For that reason, remained unmineralized matrix components are removed from the resorption lacuna. Possible candidates for this preparation of the bone surface are the bone lining cells or osteomacs [16, 20]. Concomitantly, a change from osteoclast to osteoblast activity takes place during this stage.

The formation phase is initiated by the recruitment and activation of the bone forming osteoblasts. This may be induced by soluble coupling factors that were embedded in the bone matrix and are released during bone degradation, such as transforming growth factor- β (TGF- β). Another possibility is the secretion of coupling factors by osteoclasts. Candidate molecules are for instance sphingosine 1-phosphate and ephrin-B2. Upon activation, osteoblasts become cuboidal and start to deposit new unmineralized bone matrix (osteoid). The subsequent

incorporation of osteoblast derived calcium and phosphate into the osteoid then leads to the mineralization of the new bone matrix.

Osteoblasts synthesize as much bone as osteoclasts had removed during the resorption phase. Therefore, the remodeling cycle is terminated when the initial amount of bone is reestablished. The bone forming osteoblasts either differentiate into fully mature osteocytes, quiescent bone lining cells or undergo apoptosis. Finally, the initial state of the bone surface is restored [for review see 20].

Macrophages

Macrophages develop from haematopoietic stem cells (HSCs) and are a part of the innate and the adaptive immune system. They derive from myeloid progenitor cells of the bone marrow that differentiate into circulating blood monocytes. In mice and humans, two distinct monocyte populations have been described, termed as “inflammatory” and “resident” monocytes [21].

Upon an activation stimulus like an infection, injury or inflammation, blood monocytes are recruited to the site of issue and differentiate into inflammatory macrophages [22]. They can attack, engulf and digest for instance pathogens or dying cells (phagocytosis) and subsequently trigger an immune response. Moreover, they can present antigens together with MHC molecules on their surface and thus activate T-lymphocytes. Next to this, they are also able to secrete pro- as well as anti-inflammatory cytokines [23].

A subset of the circulating monocytes in the blood migrates into the different tissues of the body and become so called resident tissue macrophages [22]. This macrophage subset together with its progenitors is considered as the mononuclear phagocyte system (MPS) [24]. They are present in nearly every tissue of the body where they constantly survey their environment. Under pathological conditions, they can get activated and participate in the establishment of an immune response [51]. Next to this immunological role, they can even take over tissue specific functions [22, 25, 26] due to tissue adaption.

The F4/80 antigen, a surface molecule of the EGF-TM7 receptor family, is mainly expressed on mature macrophages [27, 28]. Thus, an antibody against F4/80 can be used to visualize murine mature macrophages.

Osteomacs

In bone, these resident tissue macrophages are called osteomacs and can be found on the inner and outer surface of the bone. They are a profound cellular component of the bone as they make up approximately 1/6 of the total osteogenic cells and build up a huge network all over the bone surface [29].

Moreover, osteomacs are associated with sustaining HSC niches in the bone marrow. Depletion of them leads to a disruption of these niches and subsequently triggers the recruitment of HSCs into the peripheral blood [30]. Thus, they are crucial for the maintenance of hematopoiesis.

Recently it could be shown that primary osteoblast cultures, that were often used as a model system for osteoblasts, were contaminated with these resident macrophages [29]. Furthermore, they could prove that lipopolysaccharide (LPS) responsiveness in these cultures as well as accurate osteoblast function in vitro [29] and in vivo [31] depends on the co-isolated osteomacs. These findings suggest important roles of osteomacs in bone biology and make a re-investigation of several osteoblast functions observed in these cultures indispensable.

Additionally, osteomacs cover active bone modeling [29] as well as bone remodeling sites [32]. This close anatomical localization suggests some kind of interaction between osteomacs and the other involved bone cells. This hypothesis is strengthened by the observation that upon macrophage depletion active osteoblasts at bone modeling sites disappear [29]. Furthermore, at bone remodeling sites it is proposed that osteoclasts provide some kind of coupling signal to activate and coordinate osteoblast function. In contrary, bone formation takes place at bone modeling sites despite the lack of a close anatomical contact between osteoclasts and osteoblasts. This may be achieved by an osteoclast-like support provided by osteomacs. Indeed macrophages develop from the same precursor and are also able to produce factors that are thought to be involved in osteoblast-osteoclast coupling such as TGF β [33] and ephrin B2 [34].

Finally, macrophages are able to secrete a broad range of factors that can act on bone forming osteoblasts [35, 33, 36, 37] as well as on bone degrading osteoclasts [38, 39, 40, 41, 42]. The ability of the osteomacs to interact with the two major players in bone biology makes them potent candidates for participating in bone dynamics.

Proposed model of the role of osteomacs in bone modeling

Allison R. Pettit et al. reviewed the potential involvement of osteomacs in the dynamic processes in bone [32] and proposed following model for bone modeling:

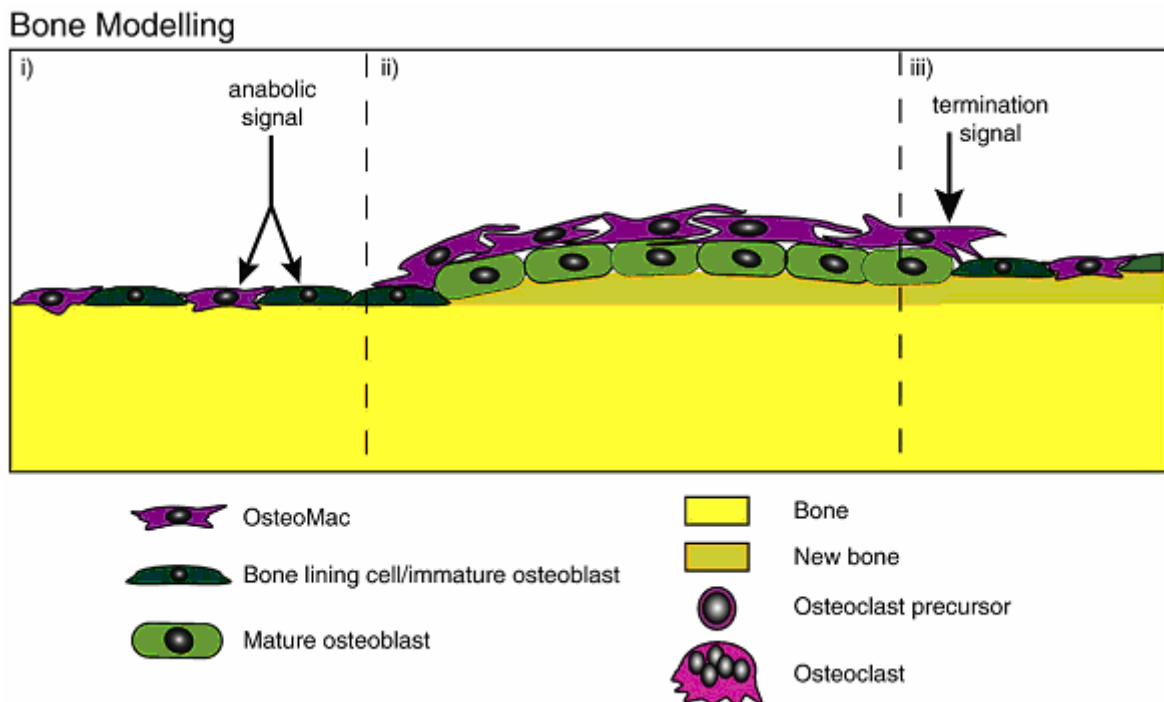


Figure 7: Proposed involvement of osteomacs in bone modelling. (Adapted from Allison R. Pettit et al. 2008)

In bone modeling, bone forming osteoblasts act independently from osteoclasts and thus reshape the structure of the bone. It is an anabolic process that is not coupled to osteoclast-mediated bone degradation.

Resting bone surfaces are covered by bone lining cells, intercalated osteomacs [29] and osteoprogenitors. As illustrated in figure 7, recruitment and proliferation of osteomacs is initiated if an anabolic stimulus is sensed by these cells. This may be achieved by M-CSF secretion by bone lining cells and osteoprogenitors. In return, osteomacs activate osteoblasts followed by the formation of a canopy-like structure of osteomacs over the bone modeling site. This leads to a close anatomical contact between osteomacs and osteoblasts. Then, osteomacs are thought to provide some kind of coupling signal to the osteoblasts that trigger the osteoid-secretion and its subsequent mineralization.

After occurrence of a termination signal or elimination of the anabolic stimuli, the initial state of the bone surface is restored.

Proposed model of the role of osteomacs in bone remodeling

Potential participation of osteomacs in bone remodeling, as proposed by Allison R. Pettit et al. [32]:

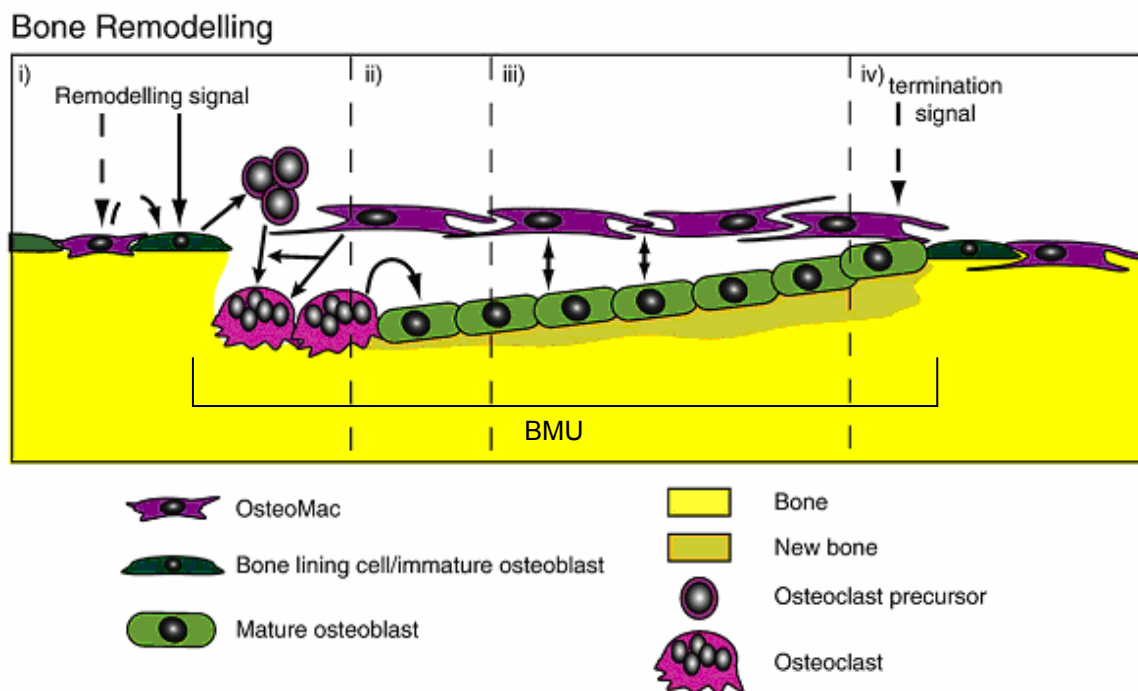


Figure 8: Potential model how osteomacs participate in bone remodelling. (Adapted from Allison R. Pettit et al. 2008)

In contrast to bone modeling, bone remodeling involves a coupled activity of bone forming osteoblasts and bone degrading osteoclasts. Therefore, the overall amount of bone tissue remains unaltered.

As indicated in figure 8, bone lining cells as well as osteomacs respond to remodeling signals by inducing the secretion of RANKL and M-CSF by osteoblasts. These two factors are crucial for the recruitment, survival and differentiation of pre-osteoclasts to mature, multinucleated osteoclasts. Concomitantly to the initiation of bone resorption, it is assumed that also osteomacs proliferate and form the characteristic canopy-structure over the bone remodeling site in response to M-CSF. At the leading end of the basic multicellular unit (BMU), osteoclasts are thought to serve a coupling signal to osteoblasts that lead to their recruitment and activation. On the contrary, they propose that the osteomacs at the tail end are responsible for regulating the ongoing osteoid secretion and late stage mineralization.

Again, either a termination signal or the lack of anabolic stimuli leads to the restoration of the quiescent bone surface.

Cathepsin S

Cathepsin S is a papain-type cysteine protease that is highly expressed in spleen and in major histocompatibility complex (MHC) class II-positive cells such as B lymphocytes, macrophages and other professional antigen presenting cells [43, 44].

Cysteine lysosomal proteases play an important role in the processing of intra- and extracellular proteins present in endosomes [45]. Furthermore, cathepsin S catalyzes the degradation of the invariant chain (Ii) to CLIP (class II-associated invariant chain peptide) and subsequently enables the peptide loading of MHC class II molecules [46]. Thus, next to other members of lysosomal proteases, cathepsin S is crucial in efficient antigen presentation.

Moreover, cathepsin S can be actively secreted from activated macrophages/microglia, maintains its proteolytic activity also at neutral pH, and is able to degrade a number of extracellular matrix (ECM) components in vitro [44, 47]. Taken together, these findings suggest that cathepsin S could also be involved in ECM remodeling.

In addition, cathepsin S favors the differentiation of mesenchymal stem cells (MSCs) to adipocytes [48]. The commitment of MSCs to either the adipocyte or the osteoblast lineage seems to be competitive [48, 49]. Thus, alterations of the amount of cathepsin S could have an influence on the fat- and bone-phenotype of an individual.

Finally, Cathepsin S knock out mice do not show a severe immunodeficiency, as numbers of B cells and T cells are normal [50]. Nevertheless, peptide loading is slowed down and germinal center reactions as well as antibody isotype switching are only weak or totally absent [50].

Hypothesis / Aim of the study

Macrophages develop from myeloid precursors that differentiate into blood circulating monocytes. A subset of these monocytes subsequently migrates into virtually all tissues of the body where they differentiate into tissue adapted, resident tissue macrophages. As cathepsin S is able to participate in ECM remodeling and is also expressed in macrophages, a knockout of this protein may influence the migration behavior of macrophages. Consequently, we hypothesized a reduced number of F4/80+ resident tissue macrophages in osteal tissues in mice deficient in cathepsin S.

After reviewing literature about the consequences of the knockout of cathepsin S, like for instance slowed down peptide loading, we expected to find a decreased MHC class II surface expression on F4/80 positive macrophages.

Preliminary data from our laboratory show that three months old cathepsin S deficient mice exhibit a discreet bone phenotype, characterized by a diminished bone mineral density. Therefore we speculated that six month old, female cathepsin S knockout mice display a decreased bone mineralization.

To investigate these ideas we performed immunofluorescence staining and flow cytometry of bone and spleen tissue of catS^{-/-} mice and wild-type mice. To examine the bone microarchitecture, micro-computed tomography analyses and histomorphometric measurements were performed on decalcified, hematoxylin and eosin stained sections.

Materials

Reagents

Accutase	PAA, CatNo: L11-007
Acetic acid 99-100%	Merck, CatNo: 818755
Calcium chloride dihydrate	Merck, CatNo: 102382
Dako-Pen	Dako, CatNo: S200230
DAPI (4'-6-Diamidino-2-phenylindole)	Roche, CatNo: 10236 276 001
di-Sodium hydrogen phosphate dihydrate	Merck, CatNo: 106580
DMSO	Sigma-Aldrich, CatNo: D2650
Entellan®	Merck, CatNo: 107961
Eosin Y solution	Sigma-Aldrich, CatNo: 318906
Ethanol absolut	Prolabo, CatNo: 20821330
FCS Gold	PAA, CatNo: A15-151
Ficoll-Paque™ PLUS	GE Healthcare, CatNo: 17-1440-03
Formaldehyde solution	Merck, CatNo: 818708
Fungizone	Gibco, CatNo: 04195780 D
Glycerol 85%	Merck, CatNo: 104094
HBSS	Gibco, CatNo: 140259
Hepes	Merck, CatNo: 10110
Hydrochloric acid 30%	Merck, CatNo: 100318
Hydrochloric acid 37 %	VWR, CatNo: 20252.290
L-Ascorbic acid	Sigma-Aldrich, CatNo: A4544
Mayer's hemalum solution	Merck, CatNo: 109249
Mowiol 4-88	Carl Roth, CatNo: 0713
Paraffin 52-54 °C	Carl Roth, CatNo: CN49.2
Paraffin 56-58 °C	Carl Roth, CatNo: 6642.5

Penicillin-Streptomycin	Gibco, CatNo: 15140-122
Potassium chloride	Merck, CatNo: 104936
Potassium dihydrogen phosphate	Merck, CatNo: 104872
Saponin	Sigma, CatNo: S-130-2
Sevorane®	Abbott, CatNo: 4456
Sodium hydroxide	Merck, CatNo: 106498
Titriplex® III	Merck, CatNo: 108418
Triton® X-100	Merck, CatNo: 108603
Trizma® base	Sigma-Aldrich, CatNo: T1503
Trypsin	Sigma-Aldrich, CatNo: T7409
Xylol	Fisher Chemical, CatNo: 10385910
α-MEM	Gibco, CatNo: 22561-021
β-glycerophosphate	Sigma-Aldrich, CatNo: G9891

Sera

Goat serum Innovative Research, CatNo: IGT-SER

Antibodies & Stains

Primary and direct conjugated antibodies

- Hamster anti-mouse **CD3e** PerCP (BD Pharmingen™, CatNo: 553067)
monoclonal, clone: 145-2C11, isotype: Armenian Hamster IgG1 κ
- Rat anti-mouse **F4/80** (eBioscience, CatNo: 14-4801)
monoclonal, clone: BM8, host/isotype: Rat IgG2a, κ

- Rat anti-mouse **F4/80** PE (eBioscience, CatNo: 12-4801)
monoclonal, clone: BM8, host/isotype: Rat IgG2a, κ

- Rat anti-mouse **MHC class II** FITC (Exbio, CatNo: 1F-621-C100)
monoclonal, clone: M5/114, isotype: Rat IgG2b

Secondary antibody

- Alexa Fluor® 568 goat **anti-rat** IgG (H+L) (Invitrogen, CatNo: A-11077)
isotype: IgG

Solutions

Decalcification solution (Tris/EDTA)

Add 10 % Titriplex® III and 3.3 % Trizma® base to ddH₂O and adjust the pH to 7.4 with 20 % ammonia.

Eosin Y working solution

Add 6 % Eosin Y solution and 0.1 % acetic acid (99-100 %) to ddH₂O.

Mowiol

Mix 6 g glycerol with 2.4 g Mowiol 4-88 in a 50ml tube and stir for 1 hour at room temperature. Add 6 ml ddH₂O and stir for one more hour at room temperature. Add 12 ml 0.2 M Tris/HCl (pH 8.5), incubate for up to 3 hours in a 50 °C water bath and stir every 20 minutes to dissolve Mowiol. Clarify by centrifugation at 5000 g for 15 minutes, aliquot the supernatant and store at -20 °C.

Osteogenic medium for cell culture

Add 5 mM β -glycerophosphate and 50 μ g/ml ascorbic acid to standard medium.

Permeabilization & blocking buffer (P & E buffer)

Add 0.1 % Triton X-100 and 10 % goat serum (add prior use) to PBS.

Saponin

Mix 10 g Saponin and 23.8 g Hepes and fill up to 100 ml with HBSS. Stir over night and filter the solution (steril). For usage, dilute 1:100 in PBS.

Standard Medium for cell culture

Add 10 % FCS Gold (heat-inactivated), 1.1 % Penicillin-Streptomycin and 0.1 % Fungizone to α -MEM.

Trypsin working solution (0.1 %)

Add 10 % trypsin stock solution (1 %) and 10 % CaCl_2 stock solution (1 %) to ddH₂O, adjust pH to 7.8 with 1 N NaOH and prewarm it to 37 °C prior use.

10 x PBS

Dissolve 27 mM KCl, 1.37 M NaCl, 15 mM KH_2PO_4 and 81 mM $\text{Na}_2\text{HPO}_4 \cdot 2\text{H}_2\text{O}$ in ddH₂O.

1 x PBS

Dilute the 10 x PBS 1:10 with ddH₂O and adjust the pH to 7.4 with 0.1 N NaOH or HCl.

1 % HCl-EtOH solution

Add 3.6 % of 37 % HCl slowly in drops to EtOH absolut.

4 % PFA

Dilute 37 % formaldehyde solution in PBS.

Methods

Animals

Six months old, female cathepsin S knockout and wild-type mice on a C57BL/6J background were used for the experiments. Cathepsin S deficient mice were kindly donated by Prof. Shi (Brigham and Women's hospital, Boston, MA) and were bred according to the Austrian laws and institutional regulations at the Medical University of Vienna, Core Unit of Biomedical Research, Division of Laboratory Animal Science and Genetics. Mice were narcotized using Sevoflurane® and sacrificed by cervical dislocation.

Paraffin embedding

To prepare the isolated vertebral columns for paraffin-embedding, they were cut in shape of maximal 0.5 x 2 x 1 cm (height x length x width) and fixed in 4 % PFA for 24 hours at 4 °C, with a medium change in-between. The bone of the vertebral columns was decalcified in decalcification solution (Tris/EDTA) for 5 days at 4 °C with daily solution changes in-between and subsequently washed with ddH₂O to remove precipitated salts. The tissue was dehydrated in an increasing alcohol series (50 %, 70 %, 96 %, 96 % EtOH and twice EtOH absolute, each step for 1 hour at room temperature) and a final incubation in xylene at 4 °C over night. For optimal infiltration of the embedding material, the biopsies were placed in three different 60 °C warm baths of paraffin (melting point 52-54 °C) for 15, 15 and 30 minutes and at the end in 60 °C warm paraffin (melting point 56-58 °C) for 120 minutes. Final embedding was performed using a tissue embedding system TES 99 (MEDITE, Burgdorf, Germany).

Sectioning

Using a sledge microtome HM 400R (MICROM International, Walldorf, Germany), 4 µm thick sections were cut, placed on Superfrost® Microscope slides (Thermo Scientific, Menzel-Gläser, CatNo: J4800AMNZ) and dried for 2 days at 37 °C.

Immunohistochemistry

All sections were examined using a Carl Zeiss Axioplan 2 microscope (Carl Zeiss Microscopy, Göttingen, Germany).

- Hematoxylin and eosin staining

Paraffin embedded sections were dewaxed in xylene for two times 10 minutes, rehydrated by a decreasing alcohol series (EtOH absolut, 96 %, 70 % and 50 %, each step 5 minutes) and rinsed with ddH₂O. Specimens were stained in Mayer's Hemalum solution for 10 minutes and washed in ddH₂O for 5 minutes. Sections were differentiated in 1 % HCl-EtOH solution for 5 minutes and washed under running tap water for 10 minutes. Counterstaining was performed by incubation of the tissue for 20 seconds with Eosin Y working solution with a subsequent washing step in ddH₂O for 5 minutes. Slides were dehydrated through 96 % EtOH, EtOH absolut and xylene (each step two times 5 minutes) and mounted with Entellan®.

- Immunofluorescence staining for F4/80

For optimal attachment of the tissue to the microscope slides, they were baked for 25 minutes at 60 °C. Specimens were dewaxed and rehydrated as described above. Antigen retrieval was achieved by incubating the sections for 10 minutes with freshly made 37 °C warm 0.1 % trypsin solution. To stop the enzymatic reaction, the slides were placed under running water for 3 minutes. Sections were washed three times for 5 minutes in PBS and afterwards rinsed with ddH₂O between each step. The amount of required reagents was minimized by drawing a hydrophobic circle with the Dako Pen around the tissue. Sections were permeabilized and blocked in P & E buffer for 30 minutes at room temperature, followed immediately without washing in-between by primary antibody incubation (rat anti-mouse **F4/80**, 1 µg/ml in P & E buffer) in a humidifier chamber at 4 °C over night. The Alexa Fluor® 568 conjugated secondary antibody (0.5 µg/ml in P & E buffer) was applied for one hour at room temperature and nuclei were

stained using DAPI (1 mg/ml in PBS) for 15 minutes. Slides were mounted with Mowiol and coverslipped.

Cell culture

For establishment of the spleen cell culture, spleens were isolated and homogenized by grinding the tissue through a sieve in 10 ml standard medium. Bone marrow (BM) cells were isolated by cutting off the ends of the femora and tibiae and flushing the bone marrow with 10 ml standard medium using a 0.5 mm gauge needle.

Osteoblast cell culture: Three million BM cells were transferred into a 12-well plate and put into the incubator (37 °C, 95 % air humidity and 5 % CO₂). Medium was changed beginning with day 5 every 2 days using osteogenic medium for cell culture. This medium additionally contained β -glycerophosphate and ascorbic acid, which induced the differentiation of the mesenchymal stem cells (MSCs) in the direction of osteoblasts.

Bone marrow/spleen cell culture: 15 ml Ficoll-PaqueTM PLUS were layered with spleen or BM cells without mixing and subsequently centrifuged for 30 minutes at room temperature at 1500 rpm without brake. The white ring between the plasma and the Ficoll-PaqueTM PLUS that contains the mononuclear cells was carefully isolated and transferred into a 50 ml falcon tube. Then the cells were washed in HBSS by centrifuging them for 10 minutes at room temperature at 1500 rpm and the pellet was resuspended in 10 ml standard medium. Cells were placed in a 6-well plate and put into the incubator (37 °C, 95 % air humidity and 5 % CO₂) for 4 hours.

Flow cytometry

Bone marrow/Spleen cells: After the isolation of mononuclear cells as described above, cells were harvested using a plastic scratch, washed as mentioned before in PBS and fixed in 2 % PFA for 20 minutes at room temperature protected from light. Then they were centrifuged for 10 minutes at room temperature at 1500 rpm and pellets were resuspended and washed in PBS. After resuspension of the pellet in PBS, cells can be stored at 4 °C. For measurement, samples were

transferred to 1.4 ml ScreenMates tubes (Thermo Scientific), centrifuged for 10 minutes at room temperature at 1500 rpm and pellets were resuspended in 0.1 % saponin buffer for membrane permeabilization. Cells were centrifuged and subsequently resuspended in 50 µl antibody dilution (anti-CD3 1:100, anti-F4-80 1:100, anti-MHC II 1:20 diluted in 0.1 % saponin buffer) and incubated for 25 minutes at room temperature protected from light. After another washing step in 0.1 % saponin buffer, cells were resuspended in 250 µl PBS and measured using the BD FACSCalibur™ flow cytometer (BD Biosciences).

Osteoblast culture: On day 12, osteoblasts were washed in PBS and detached using 500 µl accutase for 4 minutes at 37 °C. Subsequently cells were harvested using a plastic scratch and transferred to a 15 ml falcon tube. After centrifugation for 10 minutes at room temperature at 1500 rpm, the pellets were resuspended in 1 ml PBS, transferred to 1.4 ml ScreenMates tubes (Thermo Scientific) and centrifuged. Cells were stained with anti-F4/80-PE (1:100, diluted in PBS) and incubated for 20 minutes protected from light. After an additional washing step in PBS, the pellet was resuspended in 350 µl PBS and measured using the BD FACSCalibur™ flow cytometer (BD Biosciences, California, USA).

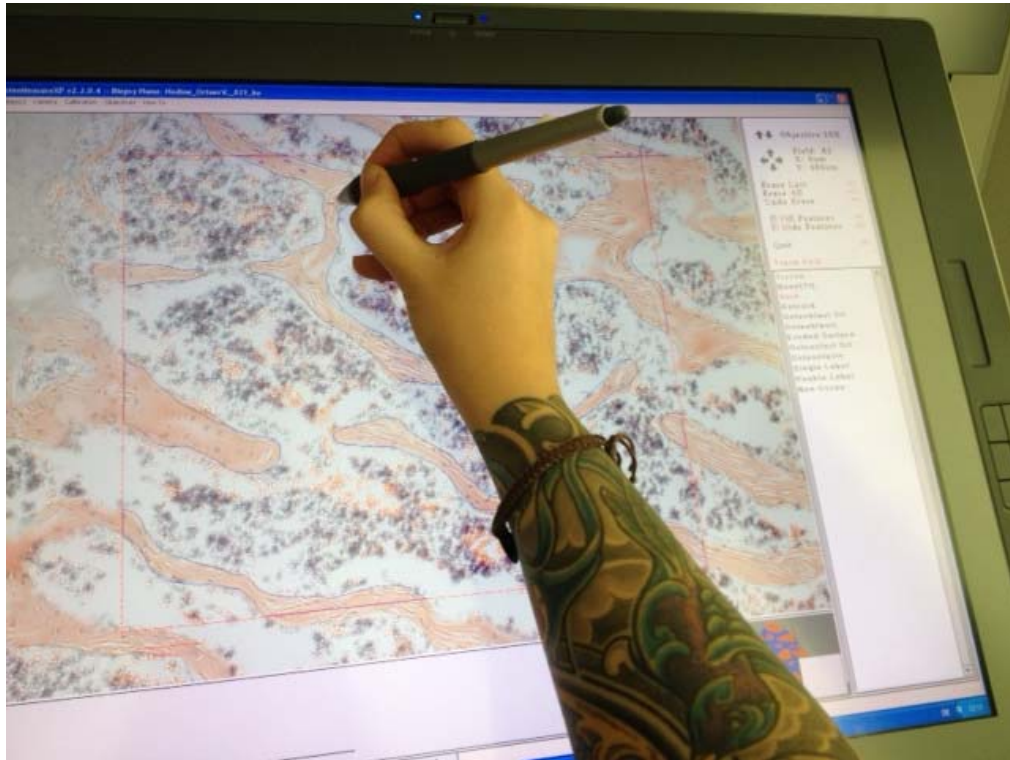
Micro-computed tomography

Vertebral columns were isolated and the fifth lumbar vertebra was measured in 70 % EtOH using the Scanco Medical µ-CT 35 (SCANCO Medical, Brüttisellen, Switzerland). In case of an inadvertent destruction of the fifth lumbar vertebra, the fourth one was used. Trabecular and cortical bone were analyzed independently from each other. Bone structures of interest were traced manually with the computer mouse. From each sample 231 slices were used for the calculation of the bone parameters.

Histomorphometry

The fifth lumbar vertebra was analyzed in HE stained sections using the OsteoMeasurexp™ (OsteoMetrics, Decatur, GA, USA). In case of an inadvertent destruction of the fifth lumbar vertebra, the fourth one was used. Sections were examined with 10x magnification on a light microscope that is connected to a

computer with the image analysis software. The borders of the trabeculae and osteocyte lacunae were manually traced with a pen on the digitized drawing tablet. Osteocyte lacunae were examined using the “void”-function of the software. Cortical bone and artifacts were excluded.



Statistical Analysis

Statistical analyses were performed using a one-sided Mann-Whitney-Test. P-values ≤ 0.05 were considered as statistically significant. All results are represented as mean value \pm standard deviation.

Results

Visualization of F4/80 positive cells

Osteomacs, the osteal resident tissue macrophages, are present in a high number in murine and human bone tissue. Due to tissue adaption they fulfill next to global, immunological functions additionally tissue specific ones. Figure 9 shows the periosteum that lines the external surface of the vertebral body. Here the osteomacs are intercalated amongst bone lining cells and osteogenic progenitor cells [3, 29]. For the visualization of these osteomacs in the vertebral column of cathepsin S knockout and wild-type mice, we used immunofluorescence stainings.

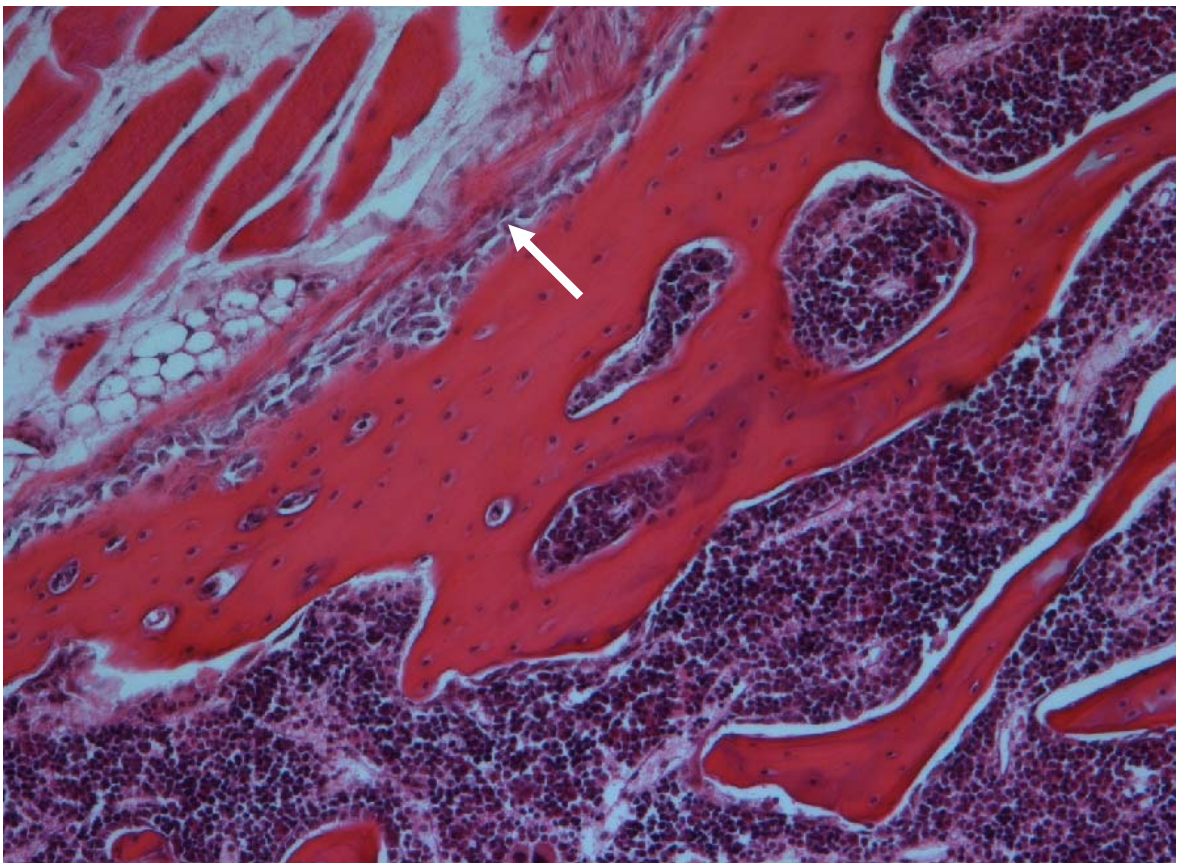


Figure 9: HE staining of the fifth lumbar vertebrae of an OF-1 mouse showing the periosteum (white arrow; original magnification: 10x). Spines were prepared as described in Figures 2 and 3. Cytoplasm and mineralized bone matrix occurs in red, nuclei in purple.

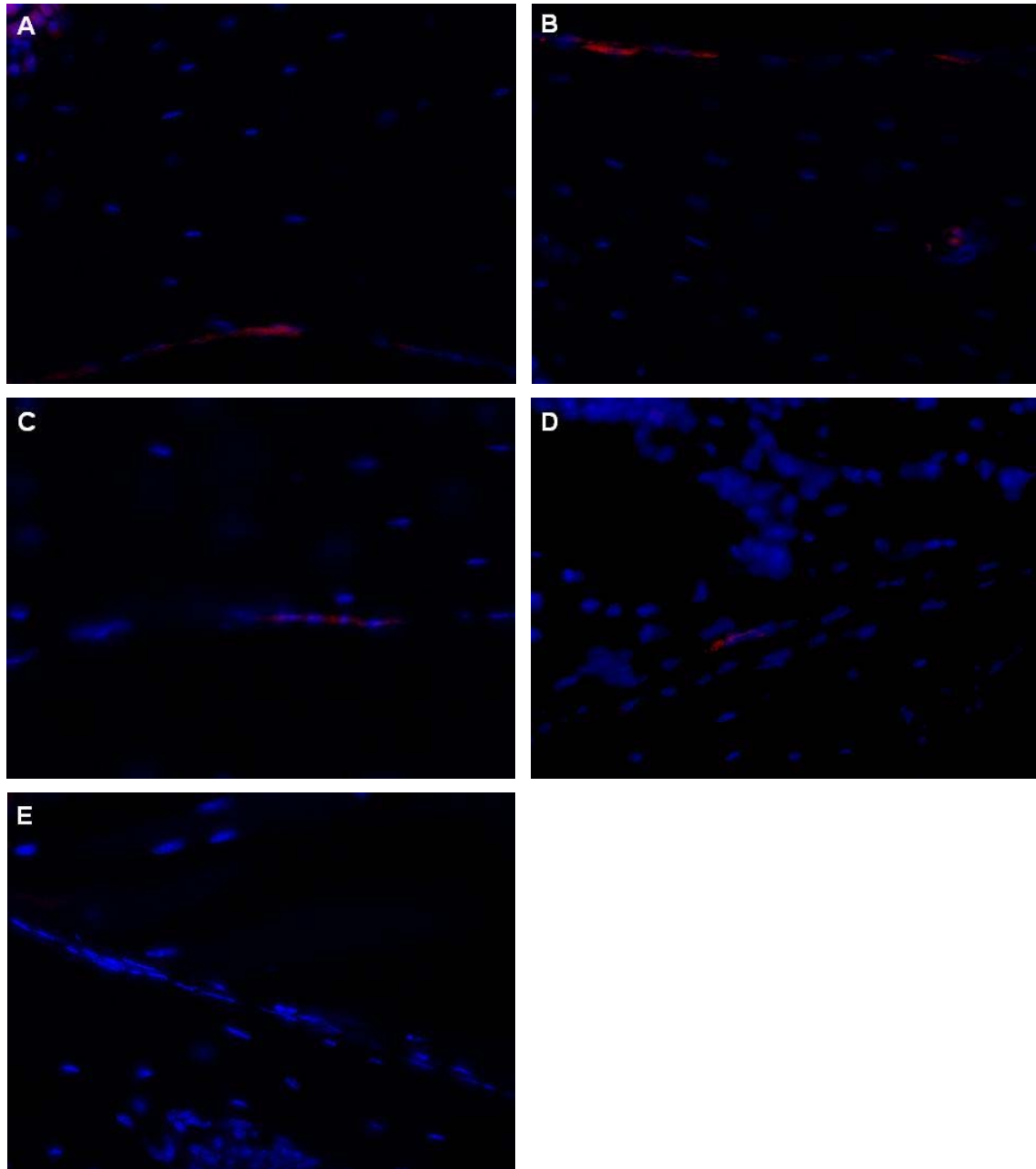


Figure 10: Osteomacs are present in the periosteum of cathepsin S knockout and wild-type mice (original magnification: 10x). A-E, Immunofluorescence staining of paraffin-embedded vertebral columns of cathepsin S knockout (A-B) and wild-type (C-D) mice. Osteal macrophages were stained with anti-F4/80 (red), nuclei with DAPI (blue). Picture E shows the negative control without primary antibody application.

Microscopic inspection did not reveal any visible differences between cathepsin S knockout and wild-type mice. The osteomacs were present in the periosteum (Figure 10, A-D) as well as on the inner bone surface lining the trabeculae. Neither the number nor the distribution and morphology of the osteomacs were changed in the knockout mice (A-B) compared to wild-type mice (C-D). Consistent with these findings, flow cytometry analysis of bone marrow cultures showed similar numbers of F4/80⁺ cells in both mouse genotypes, as shown in table 1. Also in the splenic cell cultures no significant differences in the number of F4/80⁺ cells were detectable.

Table 1: F4/80 expression in bone marrow cultures analyzed by flow cytometry.

Parameter	Wild-type (n = 3)	Knockout (n = 3)	p-value
<i>Bone marrow</i>			
F4/80 ⁺ cells [%]	4.6 ± 1.2	4.9 ± 1.8	n.s.
<i>Spleen</i>			
F4/80 ⁺ cells [%]	11.0 ± 3.2	6.6 ± 1.1	n.s.

Coisolated osteomacs in osteoblast cultures

Recently, F4/80⁺ macrophages were detected in primary osteoblast cultures derived from neonatal rodent calvaria [29]. Using flow cytometry, we proved that this co-isolation also occurs in osteoblast cultures harvested from the bone marrow of 6 month old mice.

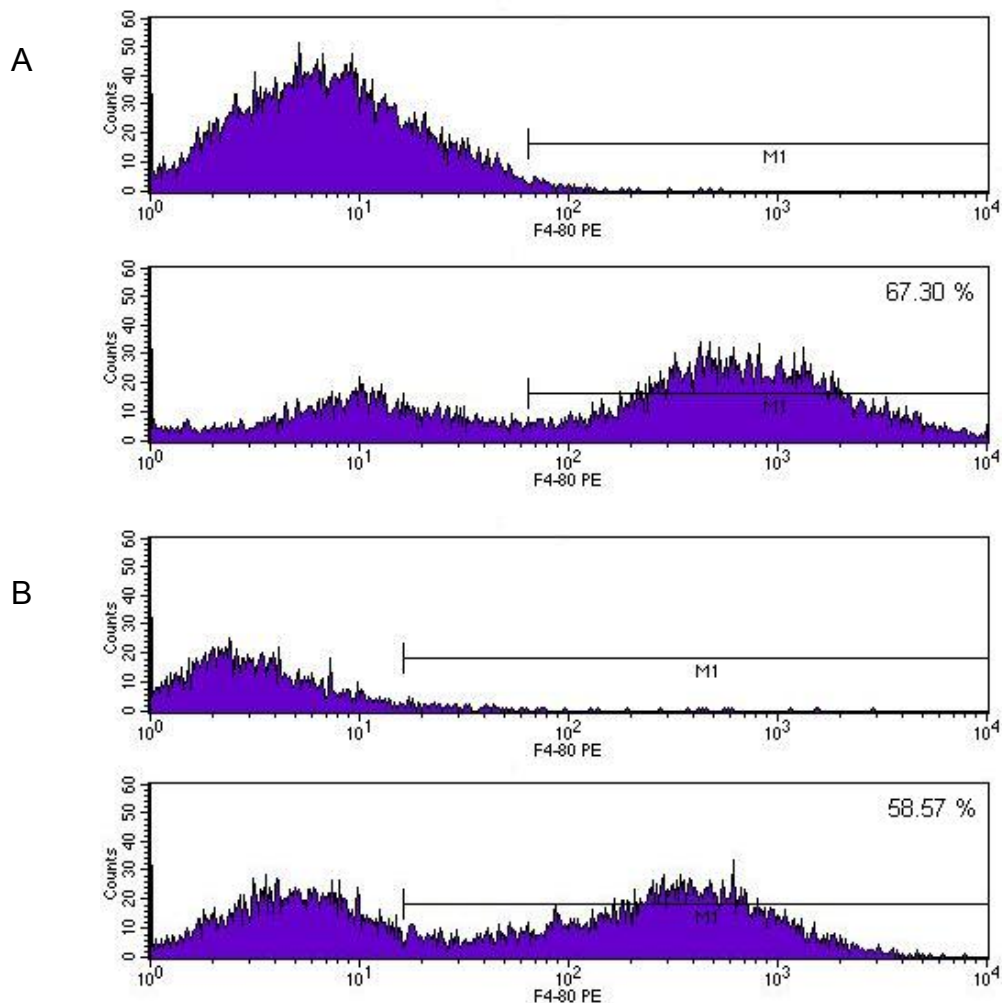


Figure 11: Flow cytometry analysis of 12 days primary osteoblast cultures from cathepsin S knockout (A) and wild-type (B) mice. Samples were stained with anti-F4/80-PE. Unstained negative controls (upper panel) were used to separate the F4/80 signal from autofluorescence. The number in the right corner represents the percentage of F4/80 positive cells in the cell culture.

As shown in Table 2, no statistically significant alteration in the portion of F4/80⁺ cells was observed. However, there was a trend in the osteoblast cultures of cathepsin S knockout mice towards an increased number of F4/80⁺ cells on day 12. The mean fluorescence intensity of F4/80 stained cells showed no relevant differences.

Table 2: F4/80 expression in 12 days osteoblast cultures analyzed by flow cytometry.

Parameter	Wild-type (n = 3)	Knockout (n = 3)	p-value
F4/80 ⁺ cells [%]	56.3 ± 6.4	69.1 ± 3.0	n.s.
MFI F4/80 [mfi]	536 ± 133	842 ± 435	n.s.

MFI = mean fluorescence intensity

Investigation of MHC II expression

Cathepsin S plays an important role in the presentation of antigens. It not only degrades proteins for this purpose, it also enables the subsequent loading of MHC II molecules on the surface of antigen presenting cells. As macrophages also express this molecule, we wanted to investigate if the lack of this lysosomal protease has an influence on the MHC II expression of osteomacs. For this purpose, cell cultures of the spleen and the bone marrow of cathepsin S knockout and wild-type mice were established. After fixation, permeabilization and staining of the cells, flow cytometry analyses were performed. Macrophages were gated using the FSC (Forward Scatter) versus SSC (Sideward Scatter) pattern and their positivity for F4/80.

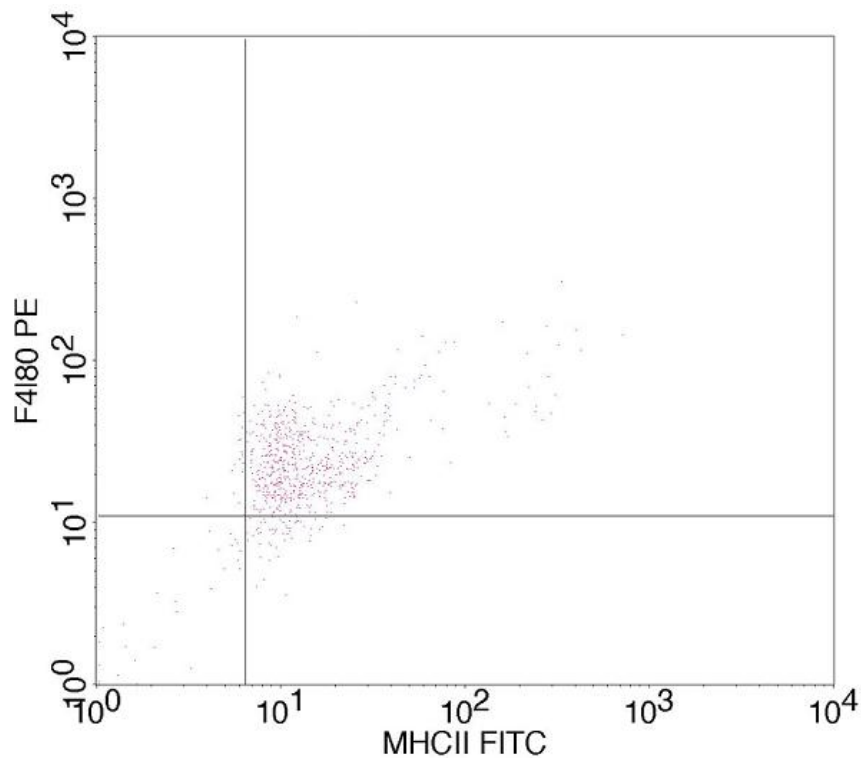


Figure 12: Dot plot of macrophages of a bone marrow culture from a cathepsin S knockout mouse. The upper right quadrant shows events that are positive for F4/80 and MHC II.

Table 3 illustrates that there was no difference in the number of MHC II expressing F4/80⁺ macrophages and in the intensity of the MHC II signal between cathepsin S knockout and wild-type mice. However, catS^{-/-} cells of both cell cultures revealed a trend towards an increased mean fluorescence intensity of the MHC II signal.

Table 3: MHC II expression of macrophages in spleen and bone marrow cell cultures analyzed by flow cytometry.

Parameter	Wild-type (n = 3)	Knockout (n = 3)	p-value
<i>Bone marrow</i>			
MHC II [%]	86.4 ± 6.5	83.4 ± 3.4	n.s.
MFI MHC II [mfi]	18.4 ± 1.2	33.1 ± 11.1	n.s.
<i>Spleen</i>			
MCH II [%]	81.7 ± 4.5	83.8 ± 4.6	n.s.
MFI MHC II [mfi]	37.2 ± 3.4	46.2 ± 4.2	n.s.

MFI = mean fluorescence intensity

Moreover, we could see two distinct subpopulations in the dot plot of mononuclear cells of the bone marrow cell culture (Figure 13, A). Both populations revealed a similar SSC pattern, a measurement for the granularity of cells. Nevertheless, they can be distinguished by their size as their FSC pattern differs from each other. In figure 13, B is shown that the smaller cells express less MHC II. As a result, we call them MHC II^{low} and the larger cells MHC II^{high}.

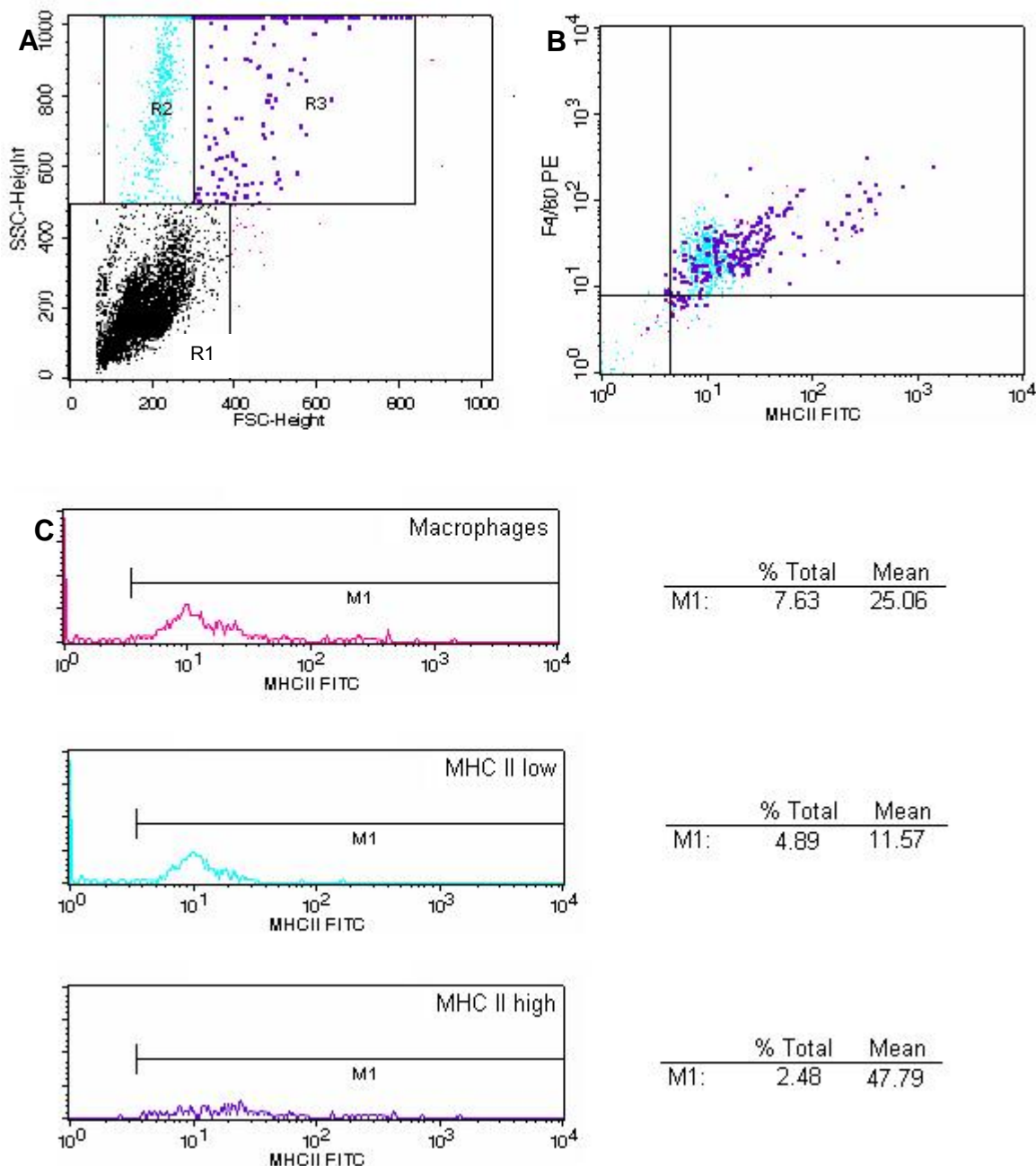


Figure 13: Bone marrow cell cultures contain two subpopulations that differ in size and mean fluorescence intensity of MHC II. A, Dot plot of the mononuclear cells of a bone marrow cell culture of a cathepsin S knockout mouse. Macrophages were defined as “not R1” and further separated into MHC II^{low} (R2) and MHC II^{high} (R3) according to their size (A) and their MHC II signal (B). C, Histograms showing the percentage of each cell population and the mean fluorescence intensity of the MHC II signal.

Table 4 demonstrates that neither the number nor the intensity of the MHC II signal of the MHC II^{low} population differs between cathepsin S knockout and wild-type mice. On the contrary, there was a significant decrease in MHC II^{high} cells in the catS^{-/-} mice. Furthermore, we observed a higher mean fluorescence intensity of the MHC II signal in these mice.

Table 4: Percentage and MHC II intensity of the two macrophage subpopulations in bone marrow cell culture analyzed by flow cytometry.

Parameter	Wild-type (n = 3)	Knockout (n = 3)	p-value
MHC II ^{high} [%]	2.89 ± 0.18	2.33 ± 0.15	0.050
MHC II ^{low} [%]	3.16 ± 0.99	3.61 ± 1.93	n.s.
MFI MHC II ^{high} [mfi]	23.33 ± 0.77	47.99 ± 3.83	n.s.
MFI MHC II ^{low} [mfi]	8.83 ± 0.73	10.62 ± 2.39	n.s.

MFI = mean fluorescence intensity

Alteration in bone microarchitecture

Cathepsin S is associated with the differentiation of mesenchymal stem cells (MSCs). As bone forming osteoblasts develop from MSCs, we wanted to investigate if cathepsin S deficiency has an effect on the microarchitecture of the bone tissue of murine vertebral columns. Therefore, we examined bone microarchitecture using x-ray based micro-computed tomography. The μ -CT scanned individual slices of an object and assembled a 3D model by laying one slice over each other. The software then analyzed the data and calculated several bone parameters.

Trabecular bone:

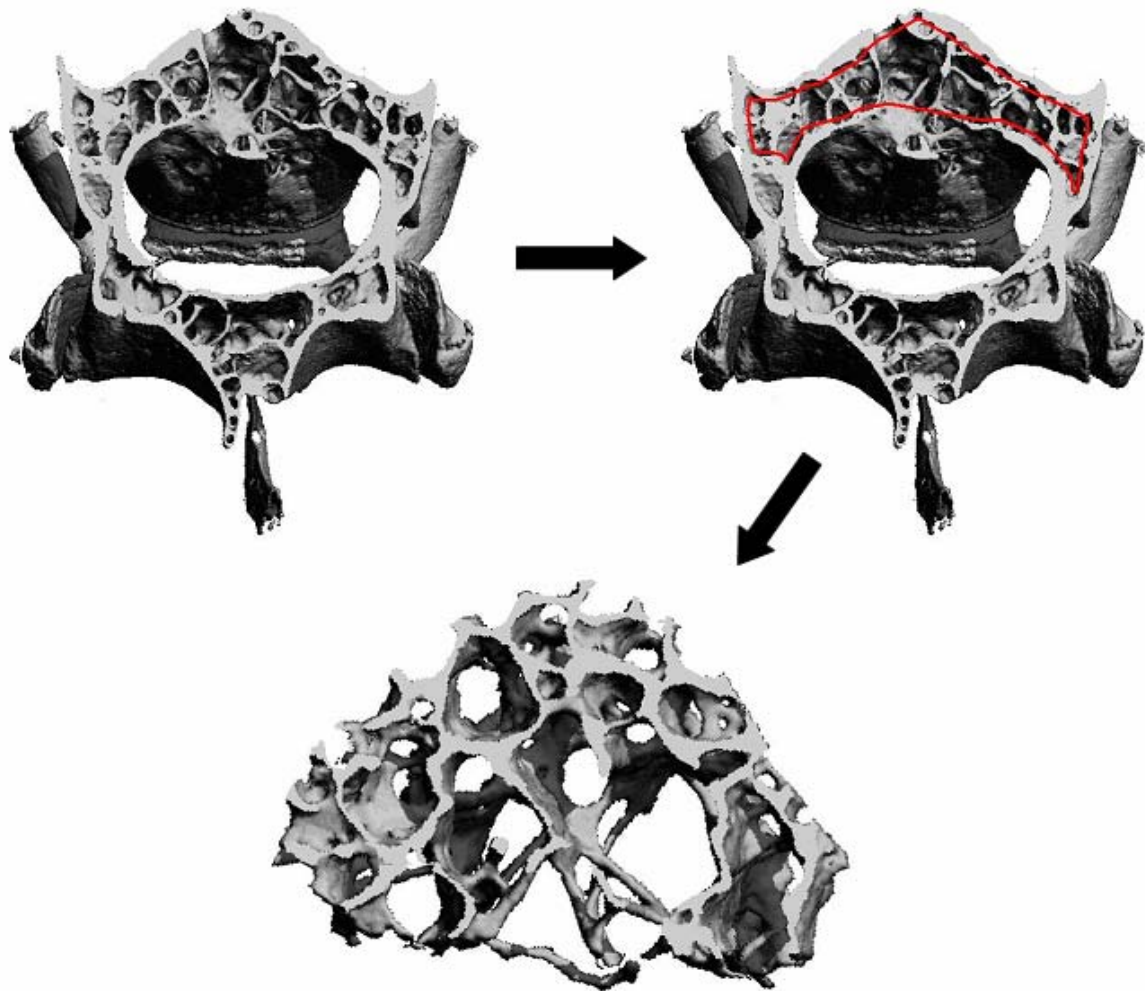


Figure 14: Manual selection of the trabecular structures of a vertebral body. The μ -CT scanned 231 slices of the vertebral body and assembled a 3D model of it. For evaluation of the trabecular bone parameters, the trabecular structures had to be selected manually on the computer.

Table 5 illustrates the μ -CT derived bone parameters of the trabecular bone structures of the fifth or fourth vertebral body of cathepsin S knockout and wild-type mice. The connectivity density gives the number of trabecular connections per mm^3 . This parameter was significantly increased in the knockout mice. Furthermore, a decrease in trabecular thickness was observed in these mice. Moreover, the tissue bone mineral density (TissBMD) parameter was decreased in knockout mice compared to their wild-type littermates. This parameter is a measure for the level of mineralization as it represents the hydroxyapatite content of the bone.

Table 5: Trabecular bone parameters

Parameter	Wild-type (n = 6)	Knockout (n = 6)	p-value
BV/TV [%]	0.23 ± 0.06	0.23 ± 0.03	n.s.
Conn. dens. [1/mm ³]	356 ± 271	666 ± 254	0.047
Tb.N [1/mm]	5.8 ± 1.4	5.4 ± 1.2	n.s.
Tb.Th [mm]	0.044 ± 0.004	0.038 ± 0.003	0.013
Tb.Sp [mm]	0.20 ± 0.06	0.21 ± 0.04	n.s.
AppBMD [mg HA/ccm]	238 ± 58	223 ± 44	n.s.
TissBMD [mg HA/ccm]	949 ± 18	915 ± 44	0.032

BV = bone volume; TV = tissue volume; Conn.dens = connectivity density; Tb.N = trabecular number; Tb.Th = trabecular thickness; Tb.Sp = trabecular separation; AppBMD = apparent bone mineral density; TissBMD = tissue bone mineral density; HA = hydroxyapatite

Cortical bone:

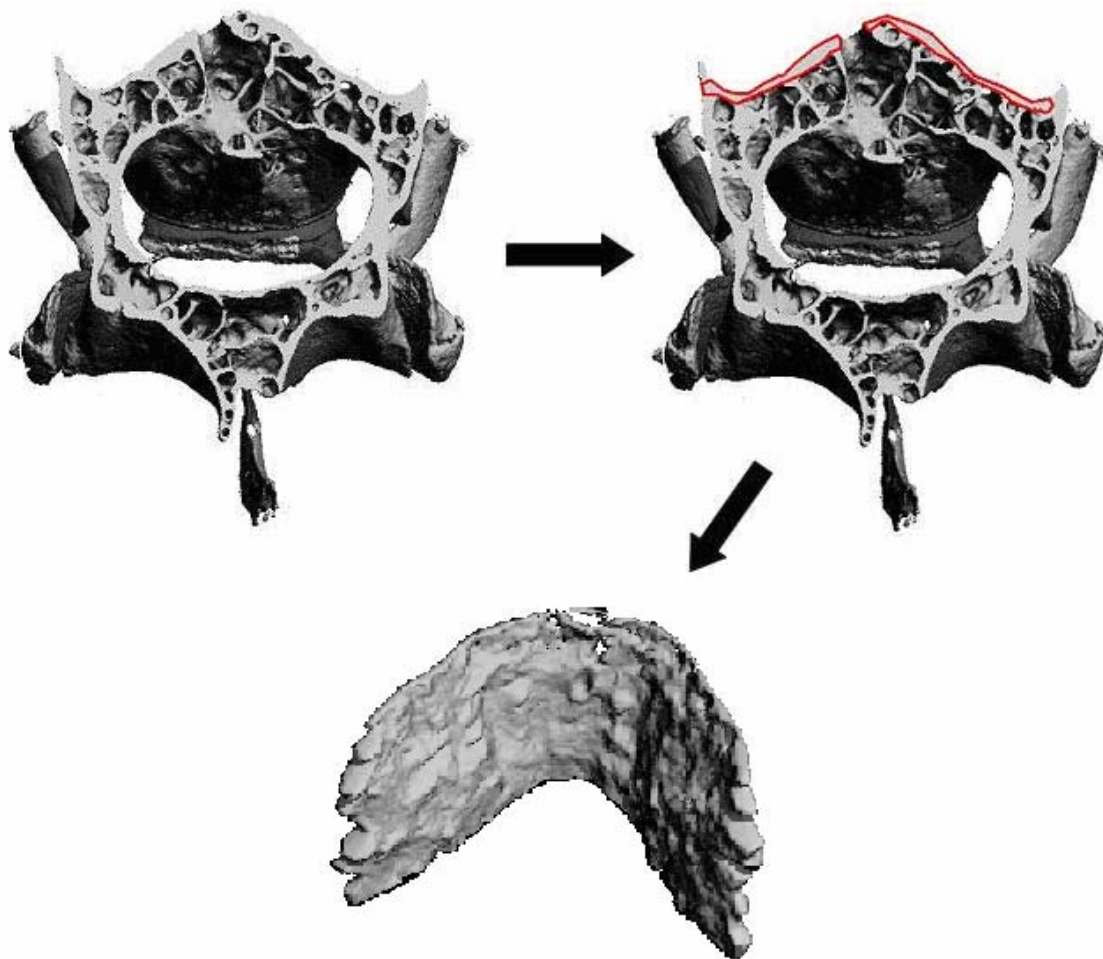


Figure 15: Manual selection of the cortical structures of a vertebral body. The μ -CT built up a 3D model of the vertebral body out of 231 scanned slices. The cortex was selected by manually tracing the borders of it on the computer.

Data of the μ -CT measurements of the cortex are demonstrated in table 6. The values of apparent bone mineral density (AppBMD) and tissue bone mineral density (TissBMD) were significantly decreased in cathepsin S knockout mice. Both parameters represent the hydroxyapatite density and therefore the level of mineralization. Apparent bone mineral density refers to bone and background, tissue bone mineral density only to bone.

Table 6: Cortical bone parameters

Parameter	Wild-type (n = 5)	Knockout (n = 6)	p-value
BV/TV [%]	0.88 \pm 0.01	0.85 \pm 0.04	n.s.
AppBMD [mg HA/ccm]	869 \pm 22	817 \pm 54	0.041
TissBMD [mg HA/ccm]	980 \pm 16	941 \pm 56	0.041

BV = bone volume; TV = tissue volume; AppBMD = apparent bone mineral density; TissBMD = tissue bone mineral density; HA = hydroxyapatite

Examination of osteocyte lacunae

A second technique to evaluate bone microarchitecture is bone histomorphometry. This 2D based technique uses stained sections of the tissue of interest. Then, tissue structures have to be manually traced on a computer drawing tablet. Several bone parameters as well as characteristics of osteocyte lacunae were calculated by the OsteoMeasureTM software.

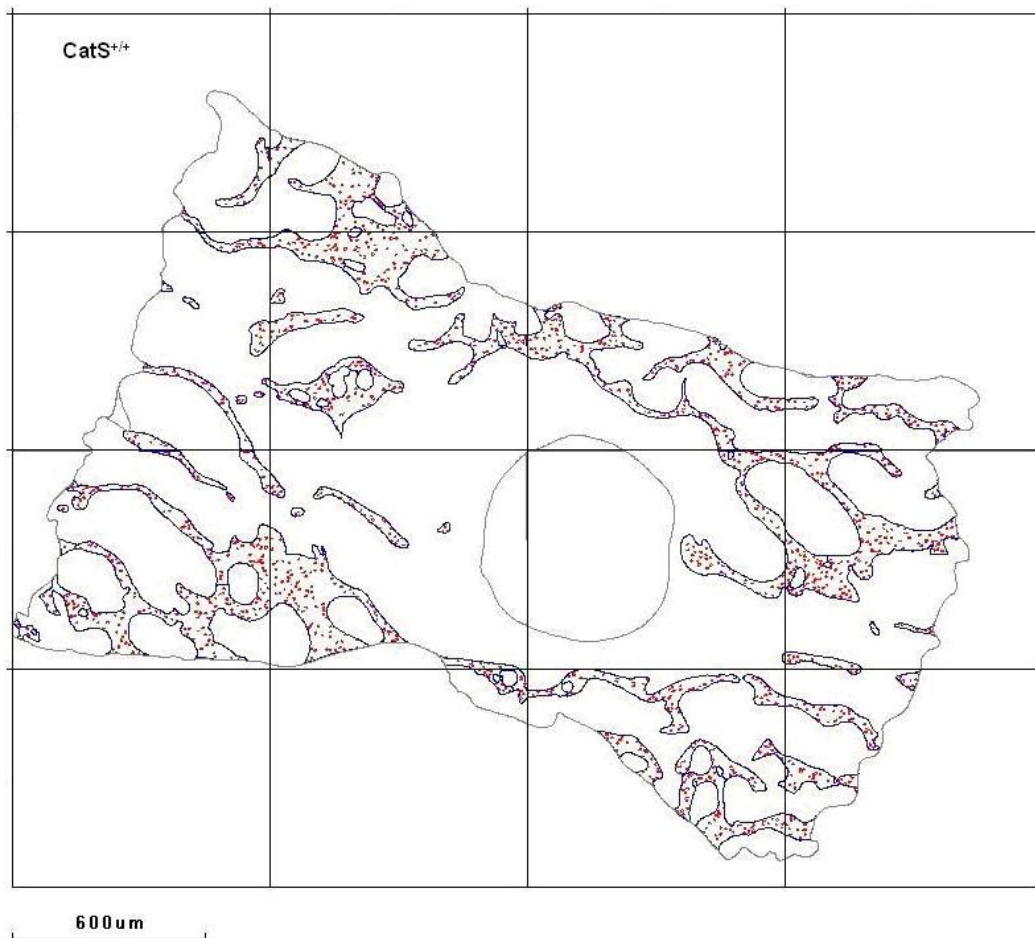


Figure 16: Overview of a lumbar vertebra of a cathepsin S wild-type mouse after manual examination. Trabecular bone is bordered in blue, osteocyte lacunae in red and artefacts (non tissue) in grey.

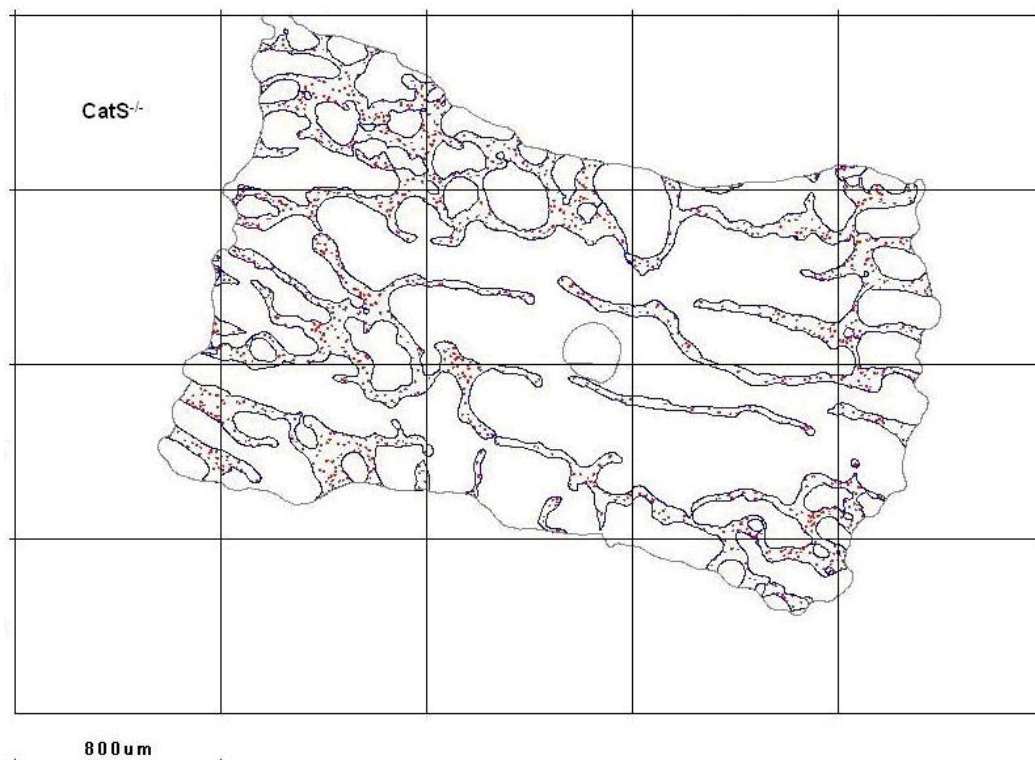


Figure 17: Overview of a lumbar vertebra of a cathepsin S knockout mouse after manual examination. Trabecular bone is bordered in blue, osteocyte lacunae in red and artefacts (non tissue) in grey.

Table 7 illustrates that there was a significant decrease in osteocyte lacuna volume to bone as well as tissue volume in knockout mice. Also the relationship of osteocyte lacuna surface to bone surface declined in the cathepsin S knockout compared to wild-type mice.

Table 7: Trabecular bone parameters, analyzed by bone histomorphometry

Parameter	Wild-type (n = 3)	Knockout (n = 3)	p-value
BV/TV [%]	19.7 ± 1.9	25.2 ± 3.5	n.s.
Ol.V/TV [%]	0.65 ± 0.02	0.44 ± 0.06	0.050
Ma.V/TV [%]	80.9 ± 1.9	75.3 ± 3.4	n.s.
BS/TV [mm ² /mm ³]	19.6 ± 1.1	18.9 ± 1.5	n.s.
BS/BV [mm ² /mm ³]	69.4 ± 42.7	75.4 ± 4.6	n.s.
Ol.S/BS [%]	38.0 ± 1.8	30.2 ± 1.1	0.050
Ol.V/BV [%]	3.31 ± 0.42	1.76 ± 0.02	0.050
Tb.Th [μm]	19.5 ± 2.0	26.1 ± 1.6	n.s.
Ol.Th [μm]	1.75 ± 0.19	1.56 ± 0.17	n.s.
Tb.Sp [μm]	82.7 ± 5.6	80.2 ± 10.3	n.s.
Tb.N [1/mm]	9.8 ± 0.6	9.4 ± 0.8	n.s.

BV = bone volume; TV = tissue volume; Ol.V = osteocyte lacuna volume; Ma.V = marrow volume; BS = bone surface; Ol.S = osteocyte lacuna surface; Tb.Th = trabecular thickness; Ol.Th = osteocyte lacuna thickness; Tb.Sp = trabecular separation; Tb.N = trabecular number

Figure 18 shows pictures of HE stained sections of three wild-type and two cathepsin S knockout mice. Microscopic inspection indicated that the number of osteocytes in the catS^{-/-} mice was diminished compared to wild-type mice. Moreover, the osteocyte lacunae appeared to be less in size. These observations were consistent with the histomorphometric results.

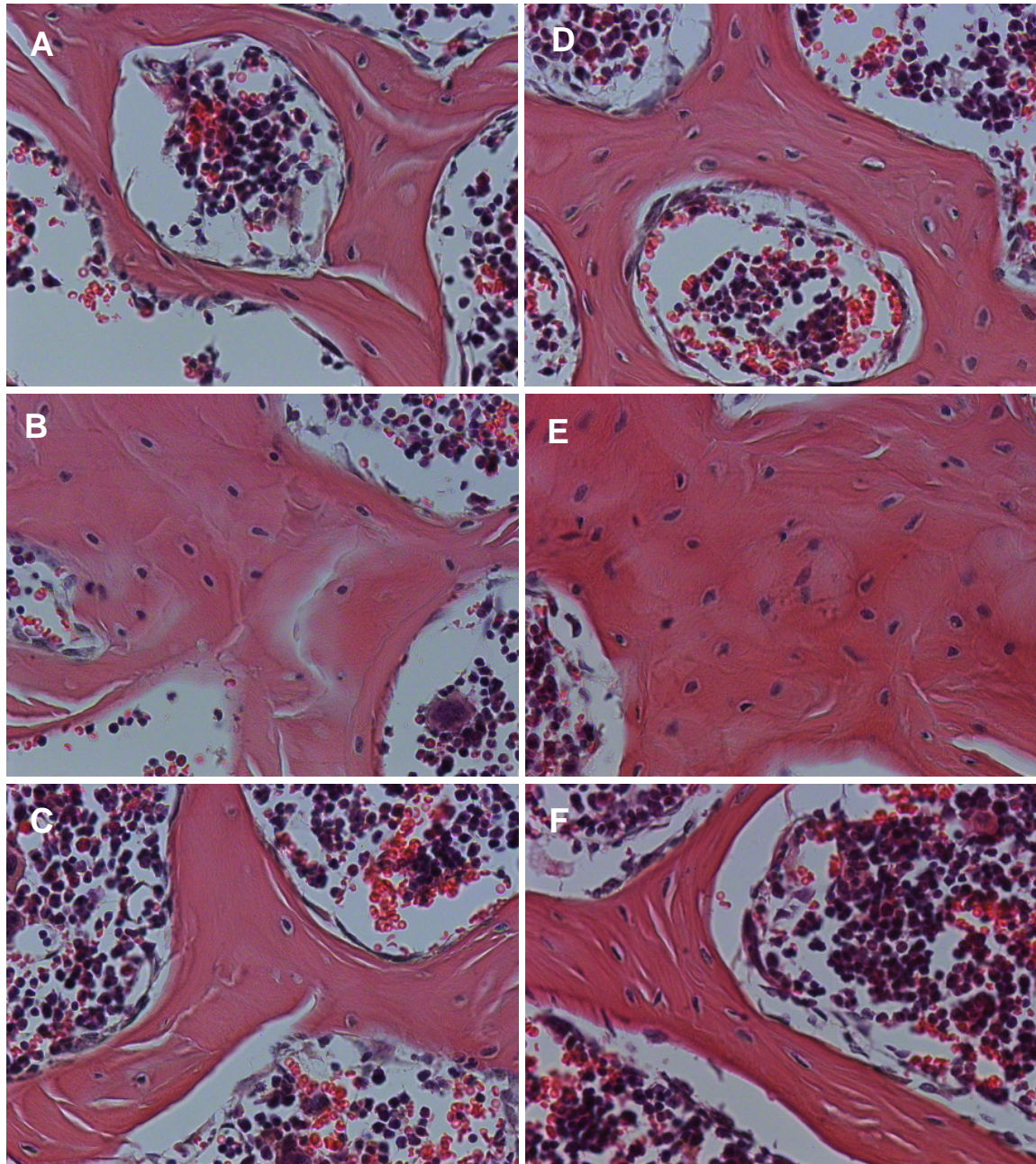


Figure 18: Osteocyte density and lacunae size in a HE stained section of cathepsin S knockout (A-C) and wild-type (D-F) mice (original magnification: 10x). Microscopic inspection confirmed the histomorphometric data about the decreased osteocyte lacunae volume in cathepsin S knockout mice. Moreover, the osteocyte lacunae appeared to be less numerous in these mice.

Discussion

Osteoimmunology is an emerging research field that focuses on the interactions between bone and the immune system [10]. Bone harbors the bone marrow and therefore provides the place for haematopoiesis [1, 30]. Thus it is crucial for the development of the cells of the immune system. On the other side, immune cells play important roles in bone biology under physiological as well as pathological conditions. One example for osteoactive immune cells are osteomacs, the resident tissue macrophages of the bone. Under physiological conditions, they support bone forming osteoblasts [29, 32]. Next to this participation in bone dynamics, they are activated by inflammatory or infectious stimuli [51]. Then they fulfill immunological functions and are able to trigger immune responses.

In the present study, we investigated the influence of cathepsin S deficiency on the presence, distribution, number and MHC class II expression of osteomacs/bone marrow macrophages. For this purpose, immunofluorescence stainings and flow cytometry analyses were performed. Moreover, bone microarchitecture was evaluated with two different techniques, μ -CT and bone histomorphometry.

Presence and distribution of osteomacs

To visualize osteomacs in the spine of wild-type and cathepsin S knockout mice, immunofluorescence stainings with a monoclonal antibody against F4/80 [27, 28] were performed. Since this surface molecule is expressed on all murine mature macrophages, also inflammatory macrophages can appear positive for F4/80. However, the localization and morphology of the stained cells in our experiments suggested that these cells belong to the resident tissue macrophage population.

They were present in both mouse genotypes and displayed a similar distribution as well as morphological characteristics. The intercalation throughout the entire periosteum demonstrated that osteomacs are a profound cellular component of the bone tissue of murine vertebral columns. Moreover, they could be found on the inner bone lining layer covering the trabeculae as well as in the bone marrow. As shown by others [30], there they fulfill essential functions in the maintenance of the haematopoietic stem cell niches.

Also on a morphological level no visible differences between wild-type and cathepsin S knockout mice were observed. The F4/80 positive cells displayed an

elongated cell body with processes reaching into their local environment. This stellate morphology together with their high number may enable the establishment of a broad network covering the whole outer bone surface. Consistent with this, the observations from Chang et al. [29] on endosteal surfaces also indicated the formation of a comprehensive network by osteomacs.

As osteomacs are required for adequate osteoblast function, they can be found in bone tissue at sites of bone formation. There they envelope active, cuboidal osteoblasts [29, 32]. Since only a small portion of the total bone tissue gets remodeled at one time point, this may not be the only reason for the extensive occurrence of osteomacs on the entire bone surface.

Another possible explanation for the high number and connectivity of osteomacs on periosteal and endosteal surfaced could be their role in immune surveillance. Analog to other resident tissue macrophage populations, like for instance the microglia in the brain and spinal cord [25], they may act as an immunological guard. For that reason, they scan constantly their local environment to quickly respond to pathological changes or inflammatory stimuli. Indeed, osteomacs were shown to respond to lipopolysaccharide (LPS) [29], a bacterial component that is able to trigger a strong immune response.

Taken together, osteomacs are clearly a profound component of the murine vertebral bone tissue. They fulfill tissue adapted physiological functions and additionally play an important role in immunological monitoring of bone tissue.

Number of osteomacs / bone marrow macrophages

Quantitative statements using immunofluorescence stainings are rather subjective. Therefore, we performed flow cytometry analyses to determine possible differences in the number of F4/80 positive cells between wild-type and cathepsin S knockout mice.

In the mononuclear cell fraction of splenic and bone marrow derived cell cultures, no statistically significant alterations in the number of F4/80 positive macrophages were observed.

As shown by Chang et al. [29], F4/80 positive macrophages can be co-isolated during the preparation of primary osteoblast cultures obtained from neonatal

rodent calvaria. Also in our cell culture preparations, harvested from flushed out bone marrow of murine femora and tibiae, F4/80 positive cells were present. Indeed, macrophage survival is dependent on M-CSF and osteoblasts are able to produce this factor [52]. Contradictory to the findings in the two other cell cultures, we could surprisingly see a non significant but distinct increase in the relative amount of F4/80 stained cells in the osteoblast cultures of cathepsin S knockout mice. Hence, there was a reciprocal reduction in the relative fraction of osteoblasts in the cathepsin S knockout cultures.

This finding would be in line with the μ -CT derived data, where we observed a diminished mineralization level of the bone tissue. As osteoid production and its subsequent mineralization is both carried out by active osteoblasts, less mineralized bone tissue indicates a dysfunction or absence of active osteoblasts. Therefore both, the reduced osteoblast number in the osteoblast cultures and the reduced mineralization state could be the outcome of an osteoblastic insufficiency in cathepsin S knock-out mice.

MHC class II expression

Macrophages are immunologically active cells that belong to the group of professional antigen presenting cells. Cathepsin S is involved in two major steps of antigen presentation. Next to other lysosomal acidic proteins it helps to degrade the engulfed extracellular material [45]. Additionally, cathepsin S enables the loading of MHC class II molecules by cleaving the peptide-binding cleft blocking molecule [46]. To examine, if the knockout of cathepsin S influences MHC class II surface expression, flow cytometry analyses of osteoblast, spleen and bone marrow derived cell cultures were performed.

In none of the three cell culture systems a significant alteration of the number of MHC class II expressing macrophages could be observed. In the descriptive statistical analysis the mean fluorescence intensity (MFI) of the MHC class II signal on macrophages in the $\text{catS}^{-/-}$ derived cell cultures was much higher than in the wild-type mice. Nevertheless, due to the chosen one-sided statistical method no statistical significance was observed. An increase in MHC class II expression despite an unchanged cell number indicated a MHC class II upregulating mechanism in cathepsin S knockout mice.

MHC class II expression is controlled in a strict manner, solely on a transcriptional level. It is expressed constitutively on professional antigen presenting cells such as macrophages, B-lymphocytes or dendritic cells. The expression of MHC class II molecules can be upregulated or even induced in MHC class II negative cells by cytokines, like for instance IFN- γ . This is achieved by the activation of class II, major histocompatibility complex, transactivator (CIITA). This positive regulator of MHC class II can be transcriptionally activated by IFN- γ , LPS, IL-4 or distinct differentiation factors. These factors act on one of the four promoters of the CIITA encoding gene (MHC2TA) what subsequently results in CIITA expression. CIITA itself binds to the enhanceosome of MHC class II and acts as a transcriptional coactivator [for review see 53]. Thus, activation of CIITA by for instance inflammatory cytokines can lead to an upregulation of MHC class II surface expression.

Indeed, unpublished data from our laboratory demonstrating an elevation of acute-phase serum amyloid A suggest that in the cathepsin S knockout mice a mild inflammation is present. This apolipoprotein is a rapidly responding reactant that is secreted during the early phase of inflammation [54]. As inflammatory conditions trigger the synthesis and release of several cytokines, this may explain the upregulation of MHC class II molecules on the surface of F4/80 positive macrophages.

Moreover, we found two distinct subpopulations in the bone marrow derived cell cultures of wild-type and cathepsin S knockout mice. These subpopulations differed in size and MHC class II expression. The smaller cells expressed less MHC class II and were therefore called MHC II^{low}. Consistent with this nomenclature, the larger and more MHC class II expressing cells were termed MHC II^{high}. The existence of a MHC II^{low} and MHC II^{high} macrophage subset has already been described in other tissues [55]. The latter ones may represent immunologically activated macrophages, as they rise in size when they phagocytose material and increase their MHC class II expression for efficient antigen presentation. Both can be induced by the presence of IFN- γ , as this type II interferon is able to act on macrophages by increasing antigen presentation and lysosomal activity [56]. The number of this MHC II^{high} cells decreased in a significant manner in mice lacking cathepsin S. In line with our original hypothesis,

this finding indicates that there is an inherent defect in catS^{-/-} mice concerning MHC II^{high} expressing macrophages.

Moreover, it could also be possible that there is a kind of a compensatory mechanism by which the MHC II^{high} cells try to balance their diminished number with increased surface expression of MHC class II molecules.

Bone microarchitecture

For the evaluation of the bone microarchitecture, murine vertebral bodies were examined by two different methods. On the one hand, we used X-ray based μ -CT analysis. It is a fast and non-destructive method that assembles a 3D model of the sample out of a number of scanned slices. Bone parameters are then directly calculated by the μ -CT software. To investigate the bone microarchitecture on a microscopic level, we additionally performed histomorphometric measurements of decalcified, hematoxylin and eosin stained sections.

Bone consists of two different compartments: cortical bone on the outside and trabecular bone that makes up the interior and harbors the bone marrow [1]. μ -CT measurements of the trabecular bone revealed a significantly decreased tissue bone mineral density (TissBMD) in cathepsin S knockout mice compared to the wild-type mice. This parameter gives the mineralization degree of the bone by examining the hydroxyapatite density of the bone tissue. Moreover, the thickness of the trabeculae was diminished in the knockout mice while the number of trabecular connections per mm³ increased in a significant manner.

Also the cortical μ -CT derived results showed a significant decrease in tissue as well as apparent bone mineral density (AppBMD) in the knockout mice. Both parameters describe the level of mineralization of bone. While AppBMD represents the hydroxyapatite density in relation to bone and background, TissBMD only refers to bone. The decreased AppBMD may suggest that in cathepsin S deficient mice intracortical porosity is increased. This age-related alteration in cortical bone microarchitecture has a major impact on the mechanical properties of bone. Thus it is a crucial risk factor for microdamages and subsequently fractures [57].

Data from the histomorphometric measurements support the picture of an impaired bone phenotype. With bone histomorphometry it was possible to assess

individual osteocyte lacuna. Compared to wild-type mice, there was a significant decrease in the overall volume of the osteocyte lacunae. Microscopic inspection of HE stained sections strengthened these observations and additionally gave the impression of a diminished number of osteocytes (Figure 18).

Taken together, the trabecular as well as cortical μ -CT derived findings indicated that cathepsin S knockout mice display a discreet bone phenotype with less mineralized bone tissue and thinner trabeculae. In addition, data from bone histomorphometry showed a decline in osteocyte lacunae size and number.

The mineralization of new bone matrix is catalyzed by active osteoblasts. Possible reasons for a diminished mineralization could be the absence or reduction of the number of osteoblasts or an impaired osteoblastic activity. Osteomacs are crucial for adequate osteoblast function and their removal leads to the disappearance of active osteoblasts at bone modeling sites [29]. If there is a negative influence of cathepsin S deficiency on osteomacs, their supportive effect on osteoblasts could be inhibited. Since osteomacs are resident immune surveillants, inflammatory or infectious stimuli could trigger a shift from the resident physiological phenotype to an immunologically active one. Indeed, as mentioned before there is an ongoing, mild inflammation in mice lacking cathepsin S. Therefore, an immunological activation of resident tissue macrophages may cause a reduction in the support of bone forming osteoblasts by osteomacs. Consequently, less osteoblasts get activated, engulfed and finally differentiated into mature osteocytes. This hypothesis would be in line with our findings, of a less mineralized bone tissue and the reduction of osteocyte lacunae size and number.

Strengths and limitations

Our work has several strengths and limitations.

The study was performed in an in vivo model of cathepsin S deficiency. In contrast to the knock-down technology, where genes are only partially shutdown, it is here possible to completely turn off a gene in an organism. Therefore influences of a remaining portion of the gene product are prevented. Moreover, two different technologies for the evaluation of the bone microarchitecture were used.

One limitation of the present study was the relatively small population size. Furthermore, the application of additional marker in immunofluorescence stainings and flow cytometry measurements would allow a more precise distinction between the inflammatory and resident tissue macrophage populations and an improved assessment of the role of osteomacs in the pathogenesis of osteoblast dysfunction. To further investigate the influence of the cathepsin S deficiency on the number of active osteoblasts, additional histomorphometric analyses have to be performed.

Conclusion

Taken together, cathepsin S deficiency led to a discreet bone phenotype that is mainly characterized by a diminished bone mineralization. Additionally, we found an inherent effect on the MHC II^{high} macrophage subpopulation, as they displayed a decreased number together with an increased MHC class II surface expression. As a result, we hypothesize the following role of cathepsin S and osteomacs in the establishment of this phenotype:

Cathepsin S deficiency causes a mild, ongoing inflammation. This inflammatory state leads to the recruitment of circulating blood monocytes that differentiate into activated, inflammatory macrophages. Concomitantly, also resident tissue macrophages are activated by the inflammatory stimuli. Therefore, they change their resident phenotype towards the inflammatory one and start to fulfill immunological functions such as antigen presentation. Subsequently, the support of bone forming osteoblasts is drastically reduced. This lack of support leads to less active, bone forming osteoblasts and therefore to a declined number of osteocytes incorporated in the bone tissue. Consequently, the bone tissue of mice lacking cathepsin S is less mineralized.

Moreover, cathepsin S may influence the early differentiation of mesenchymal stem cells (MSCs). It is proven that cathepsin S deficiency causes a decrease in the differentiation towards the adipocyte lineage [58, 59]. If there is also a direct influence on the development of osteoblasts has to be further investigated.

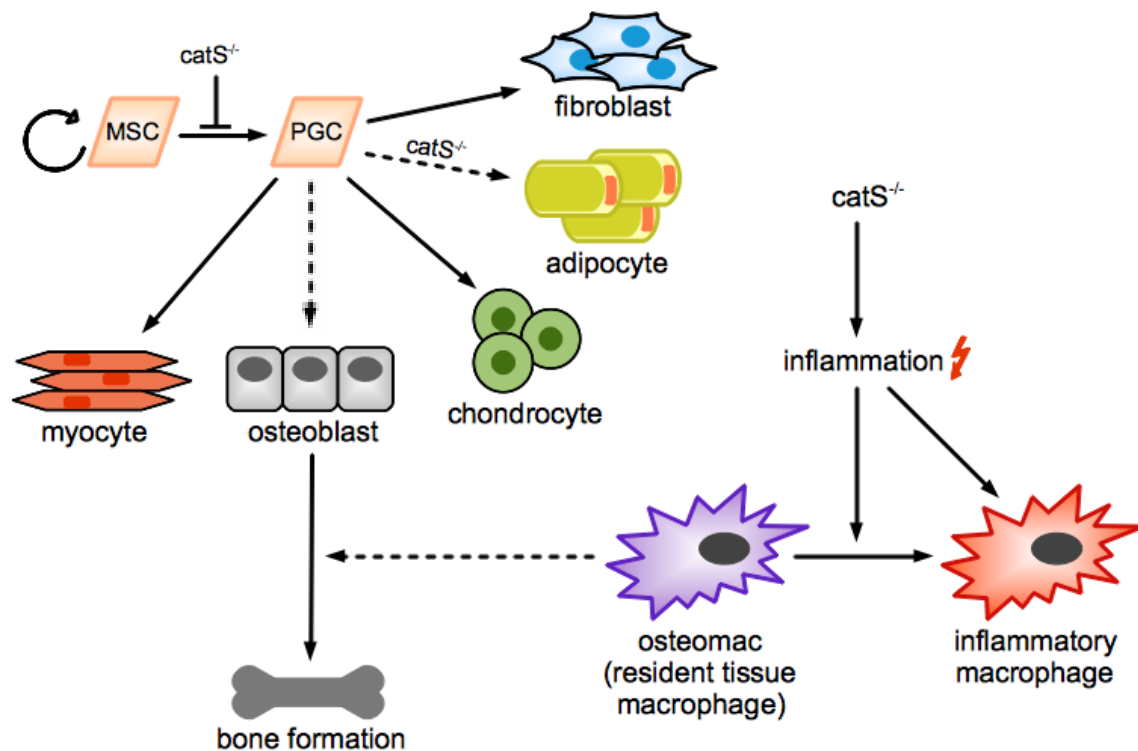


Figure 19: Proposed model of the role of cathepsin S in bone biology. Mesenchymal stem cells (MSCs) can differentiate into various cell types. Osteoblasts are the cells responsible for bone formation. This process is supported by the resident tissue macrophage population of the bone, the so called osteomacs. In mice lacking cathepsin S (*catS*^{-/-}), there may be a negative influence on the early differentiation of MSCs to progenitor cells (PGCs). Furthermore, the differentiation towards the adipocyte lineage declines in cathepsin S knockout mice. In addition, data from our laboratory suggest that in these mice a mild, ongoing inflammation is present. In consequence, circulating blood monocytes are recruited to the site of issue and differentiate into inflammatory macrophages. Moreover, resident tissue macrophages may get activated to an immunological phenotype and therefore reduce their supportive role in bone formation.

As cathepsin S favors the differentiation of MSCs towards adipocytes, it exhibits a profound pro-adipogenic effect. Moreover, it was proposed as a potent biomarker of adiposity [60]. Thus, cathepsin S seems to be critically involved in the development and pathogenesis of obesity. Therefore, the selective inhibition of cathepsin S may be a therapeutic possibility to treat adiposity, as proposed by Naour et al. [61]. Furthermore, cathepsin S inhibition in mouse models of several immune disorders such as multiple sclerosis, rheumatoid arthritis and atherosclerosis [62, 63] showed beneficial effects. Given the possible clinical relevance of the application of cathepsin S inhibitors, it has to be evaluated, if this positive effect outweighs the negative influences of cathepsin S inhibition on bone.

References

- 1) Clarke B. 2008. Normal Bone Anatomy and Physiology. Clin. J. Am. Soc. Nephrol. 3:131-139
- 2) Taichman RS. 2005. Blood and bone: two tissues whose fates are intertwined to create the haematopoietic stem-cell niche. Blood. 105:2631-2639
- 3) Allen MR, Hock JM, Burr DB. 2004. Periosteum: biology, regulation, and response to osteoporosis therapies. Bone. 35:1003-1012
- 4) Owen M, Friedenstein AJ. 1988. Stromal stem cells: marrow-derived osteogenic precursors. Ciba Found Symp. 136:42-60
- 5) Heino TJ, Hentunen TA. 2008. Differentiation of osteoblasts and osteocytes from mesenchymal stem cells.
- 6) Matsuo K, Irie N. 2008. Osteoclast-osteoblast communication. Arch. Biochem. Biophys. 473:201-209
- 7) Hofbauer LC, Heufelder AE. 2001. Role of receptor activator of nuclear factor-kappaB ligand and osteoprotegerin in bone cell biology. J. Mol. Med. (Berl). 79(5-6):243-253
- 8) Stanley ER. 1986. Action of the colony-stimulating factor, CSF-1. Ciba Found Symp. 118:29-41
- 9) Boyce BF, Xing L. 2008. Functions of RANKL/RANK/OPG in bone modeling and remodeling. Arch. Biochem. Biophys. 473:139-146
- 10) Pietschmann P. In: Pietschmann P (ed). Principles of Osteoimmunology: Molecular Mechanisms and Clinical Applications. Wien NewYork: Springer. 2001. p. V
- 11) Franz-Odenaal TA, Hall BK, Witten PE. 2006. Buried Alive: How Osteoblasts Become Osteocytes. Dev. Dyn. 235:176-190
- 12) Knothe Tate ML, Adamson JR, Tami AE, et al. 2004. The osteocyte. Int. J. Biochem. Cell Biol. 36(1):1-8

- 13) Palumbo C. 1986. A three-dimensional ultrastructural study of osteoid-osteocytes in the tibia of chick embryos. *Cell Tissue Res.* 246(1):125-131
- 14) Burger EH, Klein-Nulend J. 1999. Mechanotransduction in bone – role of the lacuno-canalicular network. *FASEB J.* 13:101-112
- 15) Chambers TJ, Fuller K. 1985. Bone cells predispose bone surfaces to resorption by exposure of mineral to osteoclastic contact. *J. Cell Sci.* 76:155-165
- 16) Everts V, Delaissé JM, Korper W, et al. 2002. The bone lining cell: its role in cleaning Howship's lacunae and initiating bone formation. *J. Bone Miner. Res.* 17(1):77-90
- 17) Miller SC, de Saint-Georges L, Bowman BM, et al. 1989. Bone lining cells: structure and function. *Scanning Microsc.* 3(3):953-961
- 18) Väänänen HK, Laitala-Leinonen T. 2008. Osteoclast lineage and function. *Arch. Biochem. Biophys.* 473:132-138
- 19) Burger EH, van der Meer JW, van de Gevel JS, et al. 1982. In vitro formation of osteoclasts from long-term cultures of bone marrow mononuclear phagocytes. *J. Exp. Med.* 156(6):1604-1614
- 20) Ragatt LJ, Partridge NC. 2010. Cellular and Molecular Mechanisms of Bone Remodeling. *J. Biol. Chem.* 285(33):25103-25108
- 21) Geissmann F, Jung S, Littman DR. 2003. Blood monocytes consist of two principal subsets with distinct migratory properties. *Immunity.* 19(1):71-82
- 22) Gordon S and Taylor PR. 2005. Monocyte and macrophage heterogeneity. *Nat. Rev. Immunol.* 5:953-964
- 23) Mosser DA, Edwards JP. 2008. Exploring the full spectrum of macrophage activation. *Nat. Rev. Immunol.* 8(12):958-969
- 24) Hume DA. 2006. The mononuclear phagocyte system. *Curr. Opin. Immunol.* 18:49-53
- 25) Davis EJ, Foster TD, Thomas WE. 1994. Cellular forms and functions of brain microglia. *Brain Res. Bull.* 34:73-78

- 26) Kolios G, Valatas V, Kouroumalis E. 2006. Role of Kupffer cells in the pathogenesis of liver disease. *World J. Gastroenterol.* 12:7413-7420
- 27) Kwakkenbos MJ, Kop EN, Stacey M, et al. 2003. The EGF-TM7 family: a postgenomic view. *Immunogenetics.* 55:655-666
- 28) Austyn JM, Gordon S. 1981. F4/80, a monoclonal antibody directed specifically against the mouse macrophage. *Eur. J. Immunol.* 11(10):805-15
- 29) Chang MK, Raggatt L-J, Alexander KA, et al. 2008. Osteal tissue macrophages are intercalated throughout human and mouse bone lining tissues and regulate osteoblast function in vitro and in vivo. *J. Immunol.* 181(2):1232-1244
- 30) Winkler IG, Sims NA, Pettit AR, et al. 2010. Bone marrow macrophages maintain haematopoietic stem cell (HSC) niches and their depletion mobilizes HSCs. *Blood.* 116:4815-4828
- 31) Alexander KA, Chang MK, Maylin ER, et al. 2011. Osteal Macrophages Promote In Vivo Intramembranous Bone Healing in a Mouse Tibial Injury Model. *J. Bone Miner. Res.* 26(7):1517-1532
- 32) Pettit AR, Chang MK, Hume DA, et al. 2008. Osteal macrophages: A new twist on coupling during bone dynamics. *Bone.* 43:976-982
- 33) Assoian RK, Fleurdelys BE, Stevenson HC, et al. 1987. Expression and secretion of type β transforming growth factor by activated human macrophages. *Proc. Natl. Acad. Sci. USA.* 84:6020-6024
- 34) Yu G, Luo H, Wu Y, et al. 2003. Ephrin B2 Induces T Cell Costimulation. *J. Immunol.* 171:106-114
- 35) Champagne CM, Takabe J, Offenbacher S, et al. 2002. Macrophage Cell Lines Produce Osteoinductive Signals That Include Bone Morphogenetic Protein-2. *Bone.* 30(1):26-31
- 36) Takahashi F, Takahashi K, Shimizu K, et al. 2004. Osteopontin is strongly expressed by alveolar macrophages in the lungs of acute respiratory distress syndrome. *Lung.* 182(3):173-185

- 37) Kreutz M, Andreesen R, Krause SW, et al. 1993. 1,25-dihydroxyvitamin D3 production and vitamin D3 receptor expression are developmentally regulated during differentiation of human monocytes into macrophages. *Blood*. 82:1300-1307
- 38) Stacey KJ, Sweet MJ, Hume DA. 1996. Macrophages Ingest and Are Activated by Bacterial DNA. *J. Immunol*. 157:2116-2122
- 39) Itoh K, Udagawa N, Kobayashi K, et al. 2003. Lipopolysaccharide Promotes the Survival of Osteoclasts Via Toll-Like Receptor 4, but Cytokine Production of Osteoclasts in Response to Lipopolysaccharide Is Different from That of Macrophages. *J. Immunol*. 170:3688-3695
- 40) Jimi E, Nakamura I, Duong LT, et al. 1999. Interleukin 1 Induces Multinucleation and Bone-Resorbing Activity of Osteoclasts in the Absence of Osteoblast/Stromal Cells. *Exp. Cell Res*. 247:84-93
- 41) van Holten J, Smeets TJM, Blankert P, et al. 2005. Expression of interferon β in synovial tissue from patients with rheumatoid arthritis: comparison with patients with osteoarthritis and reactive arthritis. *Ann. Rheum. Dis*. 64:1780-1782
- 42) Takayanagi H, Kim S, Matsuo K, et al. 2002. RANKL maintains bone homeostasis through c-Fos-dependent induction of interferon-beta. *Nature*. 416:744-749
- 43) Shi GP, Webb AC, Foster KE, et al. 1994. Human Cathepsin S: chromosomal localization, gene structure, and tissue distribution. *J. Biol. Chem*. 269, 11530-11536
- 44) Petanceska S, Canoll P and Lakshmi AD. 1996. Expression of Rat Cathepsin S in Phagocytic Cells. *J. Biol. Chem*. 271:4403-4409
- 45) Wolf PR and Ploegh HL. 1995. HOW MHC CLASS II MOLECULES ACQUIRE PEPTIDE CARGO: Biosynthesis and Trafficking Through the Endocytic Pathway. *Annu. Rev. Cell Dev. Biol*. 11:267-306
- 46) Riese RJ, Wolf PR, Brömme D, et al. 1996. Essential Role for Cathepsin S in MHC Class II-Associated Invariant Chain Processing and Peptide Loading. *J. Immunol*. 4:357-366
- 47) Shi G-P, Munger JS, Meara JP, et al. 1991. Molecular Cloning and Expression of Human Alveolar Macrophage Cathepsin S, an Elastinolytic Cysteine Protease. *J. Biol. Chem*. 267(11):7258-7262

- 48) Zhao JW, Gao ZL, Mei H, et al. 2011. Differentiation of human mesenchymal stem cells: the potential mechanism for estrogen-induced preferential osteoblast versus adipocyte differentiation. *Am. J. Med. Sci.* 341(6):460-468
- 49) Beresford JN, Bennett JH, Devlin C, et al. 1992. Evidence for an inverse relationship between the differentiation of adipocytic and osteogenic cells in rat marrow stromal cell cultures. *J. Cell Sci.* 102(Pt2):341-351
- 50) Shi GP, Villadangos JA, Dranoff G, et al. 1999. Cathepsin S Required for Normal MHC Class II Peptide Loading and Germinal Center Development. *J. Immunol.* 10:197-206
- 51) Gordon S. 2003. Alternative activation of macrophages. *Nat. Rev. Immunol.* 3(1):23-35
- 52) Felix R, Halasy-Nagy J, Wetterwald A, et al. 1996. Synthesis of membrane- and matrix-bound colony-stimulating factor-1 by cultured osteoblasts. *J. Cell Physiol.* 166(2): 311-322
- 53) Pan-Yun Ting J, Trowsdale J. 2002. Genetic control of MHC Class II Expression. *Cell.* 109:21-33
- 54) Uhlir CM, Whitehead AS. 1999. Serum amyloid A, the major vertebrate acute-phase reactant. *Eur. J. Biochem.* 265:501-523
- 55) Wang B, Li Q, Qin L, et al. 2001. Transition of tumor-associated macrophages from MHC class II(hi) to MHC class II(low) mediates tumor progression in mice. *BMC Immunol.* 12:43
- 56) Goldberg M, Belkowski LS, Bloom BR. 1990. Regulation of Macrophage Function by Interferon- γ . *J. Clin. Invest.* 85:563-569
- 57) McCalden RW, McGlough JA, Barker MB, et al. 1993. Age-related changes in the tensile properties of cortical bone. The relative importance of changes in porosity, mineralization and microstructure. *J. Bone Jt. Surg.* 8:1193-1205
- 58) Kurz M. 2012. Knochenveränderung bei Kathepsin S Knockout-Mäusen. Diploma thesis. Medical University of Vienna
- 59) Kurz M, Rauner M, Brünner-Kubath C, et al. 2011. Cathepsin S-Deficient Mice Exhibit a Bone and Fat Phenotype. *J. Miner. Stoffwechs.* 18(3):10

60) Taleb S, Lacasa D, Bastard JP, et al. 2005. Cathepsin S, a novel biomarker of adiposity: relevance to atherogenesis. *FASEB J.* 19(11):1540-1542

61) Naour N, Roualt C, Fellahi S, et al. 2010. Cathepsins in Human Obesity: Changes in Energy Balance Predominantly Affect Cathepsin S in Adipose Tissue and in Circulation. *J. Clin. Endocrinol. Metab.* 95(4):1861-1868

62) Baugh M, Black D, Westwood P, et al. 2011. Therapeutic dosing of an orally active, selective cathepsin S inhibitor suppresses disease in models of autoimmunity. *J. Autoimmun.* 36:201-209

63) Samokhin AO, Lythgo PA, Gauthier JY, et al. 2010. Pharmacological inhibition of cathepsin S decreases atherosclerotic lesions in Apoe^{-/-} mice. *J. Cardiovasc. Pharmacol.* 56(1):98-105

Abbreviations

μ-CT	micro-computed tomography
2D	two dimensional
3D	three dimensional
AppBMD	apparent bone mineral density
B cell	B lymphocyte
BM	bone marrow
BMD	bone mineral density
BMU	basic multicellular unit
BS	bone surface
BV	bone volume
CaCl ₂ ·2H ₂ O	calcium chloride dihydrate
CD	cluster of differentiation
CLIP	class II-associated invariant chain peptide
Conn. dens	connectivity density
CSF-1	colony stimulating factor-1
DAPI	4'-6-Diamidino-2-phenylindole
ddH ₂ O	double-distilled water
DMSO	dimethyl sulfoxide
ECM	extracellular matrix
EDTA	ethylenediaminetetraacetic acid
EGF-TM7	Epidermal Growth Factor-Seven Transmembrane
EtOH	ethanol
FCS	fetal calf serum
FITC	fluoresceinisothiocyanat
FSC	forward scatter

HBSS	Hank's Balanced Salt Solution
HCl	hydrogen chloride
HE	hematoxylin and eosin
Hepes	4-(2-hydroxyethyl)-1-piperazineethanesulfonic acid
HSC	haematopoietic stem cell
IFN- γ	interferon- γ
IgG	immunoglobulin G
IL-2	interleukin-2
IL-4	interleukin-4
KCl	potassium chloride
KH ₂ PO ₄	potassium dihydrogen phosphate
LPS	lipopolysaccharide
Ma.V	marrow volume
M-CSF	macrophage colony-stimulating factor
MEM	minimum essential medium
MFI	mean fluorescence intensity
MHC	major histocompatibility complex
MSC	mesenchymal stem cell
Na ₂ HPO ₄ ·H ₂ O	di-sodium hydrogen phosphate dehydrate
NaCl	sodium chloride
NaOH	sodium hydroxide
OI.S	osteocyte lacuna surface
OI.Th	osteocyte lacuna thickness
OI.V	osteocyte lacuna volume
OPG	osteoprotegerin
P & E buffer	permeabilization & blocking buffer
PBS	phosphate buffered saline

PE	phycoerythrin
PerCP	peridinin chlorophyll protein
PFA	paraformaldehyde
PMA	phorbol 12-myristate 13-acetate
PTH	parathyroid hormone
PTHrP	parathyroid hormone-related peptide
RANK	receptor activator of nuclear factor- κ B
RANKL	receptor activator of nuclear factor- κ B ligand
RT	room temperature
SSC	sideward scatter
T cell	T lymphocyte
Tb.N	trabecular number
Tb.Sp	trabecular separation
Tb.Th	trabecular thickness
TGF- β	transforming growth factor- β
TissBMD	tissue bone mineral density
TNF- α	tumor necrosis factor- α
TRAP	tartrate-resistant acid phosphatase
Tris	tris(hydroxymethyl)aminomethane
TV	tissue volume

List of figures

Figure 1: Cortical (left) and trabecular (right) bone of a murine vertebral body ...	6 -
Figure 2: Hematoxylin and eosin (HE) staining of a murine vertebral body (original magnification: 10x).....	7 -
Figure 3: HE stained section of a murine vertebra showing active, cuboidal osteoblasts (original magnification: 40x).....	8 -
Figure 4: Osteocytes lying in individual lacunae in a HE stained section of a murine vertebral column (original magnification: 40x).....	9 -
Figure 5: Bone lining cells in a HE stained section of a murine vertebral column (original magnification: 40x).....	10 -
Figure 6: A multinucleated TRAP-stained osteoclast in a bone marrow culture (original magnification: 10x).....	11 -
Figure 7: Proposed involvement of osteomacs in bone modelling. (Adapted from Allison R. Pettit et al. 2008)	15 -
Figure 8: Potential model how osteomacs participate in bone remodelling. (Adapted from Allison R. Pettit et al. 2008).....	16 -
Figure 9: HE staining of the fifth lumbar vertebrae of an OF-1 mouse showing the periosteum (white arrow; original magnification: 10x).....	28 -
Figure 10: Osteomacs are present in the periosteum of cathepsin S knockout and wild-type mice (original magnification: 10x)	29 -
Figure 11: Flow cytometry analysis of 12 days primary osteoblast cultures from cathepsin S knockout (A) and wild-type (B) mice.	30 -
Figure 12: Dot plot of macrophages of a bone marrow culture from a cathepsin S knockout mouse	32 -
Figure 13: Bone marrow cell cultures contain two subpopulations that differ in size and mean fluorescence intensity of MHC II.....	33 -
Figure 14: Manual selection of the trabecular structures of a vertebral body	35 -
Figure 15: Manual selection of the cortical structures of a vertebral body.....	36 -
Figure 16: Overview of a lumbar vertebra of a cathepsin S wild-type mouse after manual examination.	38 -
Figure 17: Overview of a lumbar vertebra of a cathepsin S knockout mouse after manual examination	38 -
Figure 18: Osteocyte density and lacunae size in a HE stained section of cathepsin S knockout (A-C) and wild-type (D-F) mice (original magnification: 10x)	40 -
Figure 19: Proposed model of the role of cathepsin S in bone biology.....	48 -

List of tables

<i>Table 1: F4/80 expression in bone marrow cultures analyzed by flow cytometry.</i>	<i>- 30 -</i>
<i>Table 2: F4/80 expression in 12 days primary osteoblast cultures analyzed by flow cytometry.</i>	<i>- 31 -</i>
<i>Table 3: MHC II expression of macrophages in spleen and bone marrow cell cultures analyzed by flow cytometry.</i>	<i>- 32 -</i>
<i>Table 4: Percentage and MHC II intensity of the two macrophage subpopulations in bone marrow cell culture analyzed by flow cytometry.</i>	<i>- 34 -</i>
<i>Table 5: Trabecular bone parameters</i>	<i>- 36 -</i>
<i>Table 6: Cortical bone parameters</i>	<i>- 37 -</i>
<i>Table 7: Bone parameters, analyzed by bone histomorphometry</i>	<i>- 39 -</i>

Curriculum vitae

Ortner Nadine Jasmin

Date of birth: 7.4.1987

Nationality: Austrian

Education

2006 – present	Molecular Biology, University of Vienna
2001 – 2006	Business College (Villach, IT-HAK)
1997 – 2001	Secondary School (Villach, St. Martin)
1993 – 1997	Elementary School (Ossiach)

Work Experience

November 2011 – present	Diploma thesis, Medical University of Vienna
April + May 2011	Center of Brain Research, Dept. Neuroimmunology
Summer 2006, 2007	Stadtmarketing Villach
Summer 2003, 2005, 2006	Magistrat Villach (Accounting)

Languages

Native German

Fluent English

Conversational Italian